10-31-1990

Photo-induced electrochemical etching of InP semiconductor in a thin film cell

Bungsu Iskandar

New Jersey Institute of Technology

Recommended Citation

Iskandar, Bungsu, "Photo-induced electrochemical etching of InP semiconductor in a thin film cell" (1990). *Theses*. 2760.

https://digitalcommons.njit.edu/theses/2760

ABSTRACT.

Title of Thesis : **Photo-Induced Electrochemical Etching of InP Semiconductor in a Thin Film Cell**

Iskandar Bungsu, Master of Science in Electrical Engineering, 1990

Thesis Directed by : **Dr. H. Grebel**

Professor of E.E. Dept.,

Optical Waveguide Laboratory.

The Photo-Induced Electrochemical Etching of n-InP wafer in aqueous solution is investigated for both reservoir and capillary systems. A sinusoidal spatial variation of light intensity pattern is directly illuminated and promoting etching on an InP semiconductor wafer. The etching process is time-efficient, and produces highly isotropical and a promising high resolution pattern. It gives a good reproducibility and has less contaminating features. Its features may be explained by a non-linear relationship between the electrolyte concentration and the photo-generated holes density at the interaction surface. An optimal reaction rate is determined by the ratio of the reactivity to ionic diffusion, either in the reservoir or capillary system. The reaction rate can be enhanced by an external biasing field at low electrolyte concentrations.

2) PHOTO-INDUCED ELECTROCHEMICAL ETCHING OF InP SEMICONDUCTOR IN A THIN FILM CELL

By

1) Iskandar, Bungsu

Thesis submitted to the Faculty of the Graduate School of
the New Jersey Institute of Technology in partial fulfillment of
the requirements for the degree of
Master of Science in Electrical Engineering
1990

APPROVAL SHEET

Title of Thesis : Photo-Induced Electrochemical Etching of InP
Semiconductor in a Thin Film Cell

Name of Candidate : Iskandar Bungsu
Master of Science in Electrical Engineering, 1990

Thesis and Abstract Approved :

Dr. H. Grebel
Professor of E.E. Dept.

Oct. 27, 89
Date

Dr. K. Sohn
Professor of E.E. Dept.

10-27-89
Date

Dr. D. Misra
Professor of E.E. Dept.

OCTOBER 27, 1989
Date

VITA

Name : Iskandar Bungsu.

Permanent address :

Degree and date to be conferred : **MSEE., 1990**

Date of birth :

Place of birth :

Secondary education : SMA Prayatna, Medan, Indonesia (1981).

Collegiate institutions attended	Dates	Degree	Date of degree
National Cheng Kung University (Tainan, Taiwan.)	1981-1985	BSEE	Jun. 1985
NJIT	1988-1989	MSEE	Dec. 1989

Major : Electrical Engineering.

Publication : 1. H. Grebel, B. Iskandar and K.G. Sheppard.
Photoelectrochemical Etching of InP in a thin Film cell.
To be published in Appl.Phys.Let, 1989.

2. H. Grebel, B. Iskandar and K.G. Sheppard.
The Effect of Non-Linear ion Transport on the Rate of Laser Induced Electrochemical Etching of Semiconductor.
To be published in J.Appl.Phys, 1989.

Position held : Research Assistant, Optical Waveguide Laboratory, Electrical Engineering Department, NJIT.

In memorial of my father

and

Dedicated to my mother.

TABLE OF CONTENTS

LIST OF FIGURES

CHAPTER 1 INTRODUCTION

Structural Etching on the semiconductor surface means a selective patterning process which removes certain portions of the semiconductor surface. Various etching techniques of the semiconductor surface have been developed today, with their advantages and prominent roles.

Conventionally, the etching of the semiconductor surface [1] may be accomplished by having a photoresist layer deposition, masking and exposing the masked sample to light. After photoresist development, a relief structure with the specific geometry patterns on the semiconductor surface is created. This process is time consuming and care should be taken for a proper mask alignment.

For the next generation of the advanced semiconductor devices with a submicrometer range of components, such as *DFB Lasers,* or *DFR Lasers,* a new efficient microfabrication technique which is less susceptible to the mask misalignment and which bears the potential of co-deposition, as well as etching, is required.

A Photo-Induced Electro-chemical Etching is one of the newly introduced technologies now being investigated. In this technique a beam directly impinges onto a semiconductor surface, where a selective composition electrolyte is sprayed on. Typically, the grating patterns, such as used in **DFB Laser**, may be produced holographically [2], i.e an optical interference pattern is introduced directly and etched onto the semiconductor wafer surface without any intermediate photoresist steps. A short wavelength laser beam is used to obtain a promise of high quality and high resolution pattern at the order of the optical wavelength.

The advantages of this technique are : etching with neutral species, material selectivity, maskless and photoresistless process with apparent cost reduction; time efficiency and reduction in the fabricating process steps; direct monitoring of the pattern formation; reduction in electrical damages; low-temperature liquid-phase technique and reduction in possible wafer contaminations. It also offers several features for controlling the high resolution etching process and modifying the material surface properties as the process proceeds. Some of these features are as follows :

- Short optical wavelength source is used, permitting submicron feature resolution.
- High ultraviolet absorption coefficient for most III-V materials means small penetration depth and a better etched-depths control.
- Photons energy are sufficiently high to produce single step excitation or bond breaking in many molecules, promoting high chemical reactivity.
- Short exposure time (order of minutes) and low incident energy, which limits the physical extent of thermal damage during

exposure.

- Enhancement of the chemical reactions and desorption of products at the surface without ion bombardment, therefore reducing surface damage compared with other etching processes.
- A broad-band incoherent light source may be used, so large areas can be processed rapidly.
- Good reproducibility of the pattern formation because it may be monitored during the exposure.

Our interest here is to reveal the behavior of the etching mechanisms under radiation from a light source, strictly speaking, an electrodeless process, electrolyte and external biasing field effects. The experimental parts will cover the etching time and etching process due to *the effect of the electrolyte concentration, both for thin capillary layers system and reservoirs (bulk electrolyte cells) system, incident laser power effects, the external electric-field effects, and the detection of the grating depth growth.*

In this thesis, I am reporting on the photo-induced electrochemical etching of n-InP wafer. The experimental results are accompanied by a simple but straightforward model to explain the findings. A grating pattern was used in order to record the resolution stability and monitor the etching process.

Since the resolution of the patterns are of interest, an on-line etching monitoring system is introduced and is accomplished by detecting the first order diffracted intensity from the pattern as it is being etched.

CHAPTER 2 BACKGROUND PERSPECTIVE

2.1 Principle and Technique of Etching.

2.1.1 Background.

Most etching processes involve one or more chemical reactions. The etching process proceeds if and only if the specimen is soluble in the etchant medium, or at least is carried away from the specimen surface by the etchant medium. The etching is, therefore, an *oxidation-reduction (Redox)* process.

The redox etching process involves a conversion of the material being etched to a soluble higher oxidation state. There are various ways of etching techniques depending upon the material to be etched, the surface patterns requirement, the necessary etching reagents, and some other factors such as economical considerations. Several etching techniques have been extensively used, such as : Immersion etching, spray etching, electrolytic (wet) etching, gas phase etching, chemical-mechanical polishing, and the novel achievement techniques including optical lithographic (such as : electron beam, X-ray and ion beam milling lithographies) [1] and *the photo-Induced Electro-Chemical Etching* [3,4,5,6].

Immersion etching (or wet chemical etching) is the simplest technique, where the masked or unmasked sample is submerged in the etched solution. In order to improve the uniformity and etching process (such as keeping the surface with fresh solution, avoiding local overheating in case of exothermic reactions), an external mechanical agitation is needed. Also, a surface active agent to the etched solution is required to prevent the bubble gas (usually H_2) accumulated on the surface. A spray etching, basically, is the same as immersion, but fresh etchant is rapidly and constantly supplied to the reaction site, while reaction products are continuously removed. This technique has a better process control and uniformity over the immersion and usually is useful for generating patterns that are relatively thick films, especially if steep pattern walls are required. Electropolishing of metals and semiconductors are examples of electrolytic etching. The rate and selectivity of etching can be controlled by the external potential and/or current density applied. The major disadvantage of wet chemical etching for patterns transfer is the undercutting of the layer underneath the mask, resulting in a loss of resolution in the etched patterns. In practice, for an isotropic etching, the film thickness should be about one third or less of the resolution required [1]. When a relatively defect-free surface is required, the combination of a slow liquid chemical surface etching with a gentle mechanical abrasion to continuously remove the products from etching reaction surface are preferred. All the above etching techniques are slow and not appropriate for the submicrometer range resolution.

2.1.2 Optical Lithography.

For an advanced micrometer range component, the optical lithography technique [1] becomes more reliable and promising. Basically, a thin layer of radiation sensitive (photoresist) material is covering the semiconductor surface, then a pattern is masked over the photoresist (either positive or negative) material. After exposure to the light, the pattern masked will be retained on the surface (for positive photoresist), and other portions are etched away. Various optical lithography methods have been studied.

In electron beam lithography, an electron gun that generating a suitable current density is focused by condenser lenses. The beam blanking plates (used to turn the electron beam on and off) controlled by a computer, direct the focused electron beam to any location in the scan field on the semiconductor [7]. This method has an advantage in the generation of micron range resist geometries. It also offers high automated and precise controlled operations. This method has a greater depth pattern and can direct patterning on a semiconductor wafer without using a mask. The disadvantages are that the resolution is limited by the electron backscattering to about 0.5 μm, registration of 0.2 μm, and low throughput [1]. The resolution is defined here to be the minimum pattern feature dimension that can be transferred with high fidelity into a resist film, registration is a measurement of how accurately patterns on successive masks can be aligned with respect to the previously defined patterns, and throughput is the number wafer that can be exposed per hour for a given mask level.

X-ray lithography offers a better resolution and higher throughput because it uses parallel exposure, as opposed to the serial exposure approach of electron beam lithography. An electron gun is incident upon a palladium target that emits an X-ray, then the X-ray emitted pass through a beryllium window into a helium-filled chamber and the X-ray masked wafer. The X-ray mask and semiconductor wafer are first well-aligned with respect to each other before being moved to the exposure position. The construction of the X-ray mask is much more complicated. The resolution is better than 0.5 μm, and 0.5 μm registration.

Ion milling lithography can offer the highest resolution nowadays (about 0.2 μm or better), since ions have a higher mass and thus scattered is less than electrons. But this technique still suffers several limitations, such as time inefficiency, cost consuming, diffraction effects and beam deflection difficulties.

2.1.3 Photo-induced Electrochemical Etching.

The photo-induced electrochemical etching has been extensively studied for the next submicrometer generation of advanced semiconductor devices [3,4,5]. Basically, The same theoretical background is being considered. The major differences are the system and the consideration parameters. In those reports, the sample was mounted as an electrode and electrically biased with a calomel electrode, and the experimental were focused on the transport carrier density generated at the interface. The system reported here is much more simple but still controllable. The electrodeless system (without using calomel electrode cell) proceeds with a direct impinging of the beam pattern onto the semiconductor surface.

In the photo-induced electrochemical etching on a semiconductor surface, the etching reaction occurs by an oxidative decomposition reaction induced by the *photo-generated* electron-hole pairs which are controlled by an incident laser beam intensity on the semiconductor surface, as well as by *the electrolyte composition* and concentration. The photo-induced electrochemical etching process may proceed if :

(1). The electrolyte can assist the oxidation reaction and dissolve the oxide species fast enough before the other processes will take place.

(2). Sufficient quantity of electron-hole pairs carriers exist within a short distance from the semiconductor surface, so that the carriers may reach the interface and participate in the reaction before the other processes, such as carriers recombination, destroy them.

(3). Also there should be sufficient photons energy to break chemical (atomic) bonds in order to promoting the oxidation reactivity. It has been estimated that the ratio of In and P atom removed from the semiconductor surface to the number of incident photon

(in case of incident optical power 6 mW) is about 10^8 - 10^9.

This quantum yield means that a relatively high absorption coefficient is required for the photon flux to produce a sufficient number of electron-hole pairs in a near surface region. The absorption coefficient magnitude should occur for the photons with energy equal to or in excess of the direct band gap of InP. The visible wavelength photons possess energy ($E = h\nu$) in excess of the band gaps of InP at the room temperature 300°K (1.35 eV).

The photo-induced electrochemical etching mechanisms on the n-type semiconductors involve four essential steps. These are :

1. The holes are created due to optical excitation.
2. The reactants are transported to the semiconductor surface, i.e. by diffusion.
3. Chemical reactions occur at the semiconductor surface, leading to the formation of oxides on the interface.
4. The dissolution of the oxides at the electrolyte-specimen interface (semiconductor surface) are transported away, i.e. by diffusion.

The etching process proceeds by oxidation, ended with the dissolution of the oxide by a chemical reaction. When the specimen-electrolyte interface is illuminated by, say, the interference of the two laser beams (hereafter, the illumination refer to the interference of the two laser beams to form the gratings pattern), the photo-generated holes at the interface are created according to the rate of the sinusoidal intensity variation (see also Eq. < 3.2.2 >). The oxidative decomposition reaction can be written as follow :

$$InP + X\,h\nu \longrightarrow InP + X\,h^{+} + X\,e^{-}$$
$$InP + X\,h^{+} \longrightarrow In^{3+} + P^{3+} + (\,6 - X\,)\,e^{-} \qquad <\,2.1.1\,>$$

Where h^{+} is the photo-generated holes and e^{-} is the electrons injected into the specimen, and $h\nu$ is the photon energy. In^{3+} and P^{3+} are the ions dissolved in the electrolyte. The photo-generated electrons would drift into the bulk of the specimen to complete the reduction reaction. Thus the illumination effect is to generate the reaction-driving electric force.

2.2 Factor Affecting Photo-Induced Etching Reaction.

The photo-induced electrochemical etching of the semiconductor surface processes may be initiated by promoting the semiconductor from its initial oxidation state to some higher oxidation states, given as Eq. < 2.1.1 > . In these equations, the holes (h^{+}) are primarily optically generated. The optical excitation of holes depends on the incident photons (which possess photon energy that is larger than the etched material band gap energy, E_g) at the semiconductor surface. The number of photons generated due to P_{op} optical incident power is

$$n_p = \frac{P_{op}}{h\nu} \qquad < 2.2.1 >$$

Where n_p is the number of photons created and $h\nu$ is the photon energy ($E > E_g$). These photons may generate the hole-electron pairs which participate in the redox reaction. So we may consider only the *incident laser power (P_o)*, with photon energy larger than the material band gap, E_g, one of the photo-induced electrochemical etching parameters.

We consider the electrolyte concentration and composition to be a direct factor affecting the etching process (etching time). The electrolyte composition may determine the dissolved species formation. The last step of the photo-induced electrochemical etching process is to transport away the dissolved species under chemical reactions. Thus, the dissolution reaction velocity may depend upon the formation of the dissolved species (solvent-crystal molecular interaction) and the dissolved species reactivity. The dissolved species (oxide composition) formation depends on the solvent used, sample preparation procedure, etc [8]. So *the electrolyte concentration (C_o) and composition* are the photo-induced electrochemical etching parameters.

The adsorption process may be considered to affect etching kinetics. Adsorption of the electrolyte (reactants) solution onto the specimen may create surface complexes which will facilitate the etching process. However, some adsorption of non-reactive species or formation of passivating surface film may slow down the etching time. Also, certain types of impurities in the electrolyte solution may be adsorbed on the specimen and hinder the etching process. Thus the specimen preparation prior to the etching process and the selectivity of electrolyte are a significant procedure.

If the photo-induced electrochemical etching of the semiconductor surface is a matter of lowering the surface potential barrier, then applying the *external potential or inducing an external electric-field* may, of course, affect the creation and activation of the holes that are needed in the etching process. The induced field determines the probability of a surface occupied state, and the surface state facilitates the etching reaction. Thus externally applied potential can control the surface reaction rate. Other factors, such as doping level, dopant etc., that are affecting the process surely may relate to the etched material.

2.3 Diffraction Grating.

One of the advantages of photo-induced electrochemical grating etching is that it permits *in situ* monitoring of the grating formation; thus the process can be interrupted whenever the gratings depth (modulation) is at a maximum or at the desired value.

The detail laser interferometric arrangement used to produce the gratings is shown in Fig. 4.1 (see p.41). For the beam incident with an ideal sinusoidal phase grating will be scattered into a various diffracted order ± m, with an efficiency of [9]

$$\eta = \frac{I_m}{I_i} = J_m^2 (\varphi) \qquad < 2.3.1 >$$

Where Im is the intensity of the m^{th} diffracted order, $J_m^2(\varphi)$ is the m^{th} order Bessel function and Ii is the incident beam intensity. The diffracted beams that were monitored for the perfect sinusoidal grating formation, follow the grating equation of

$$\sin \theta_m = \sin \theta_i - m \frac{\lambda}{d} \qquad < 2.3.2 >$$

Where d is the grating period and λ is optical source wavelength. θ_m is the m^{th} order diffracted angle and θ_i is the incident angle. The surface relief Δh produces a corresponding *phase modulation* in the diffracted beams from the sample related to

$$\varphi = \frac{2 \pi n_e \Delta h}{\lambda \cos \theta_i} \qquad < 2.3.3 >$$

Where Δh is the grating depth formation, λ is the optical wavelength, and θ_i is the incident angle.

Thus, direct monitoring of the diffracted efficiency in a real time can provide in situ measurements of the etching rate and the grating modulation amplitude. The data recorded should be corrected for the effect of the gaussian distribution in the laser beam [10] and the quantum efficiency of the photo-induced electrochemical etching process [11].

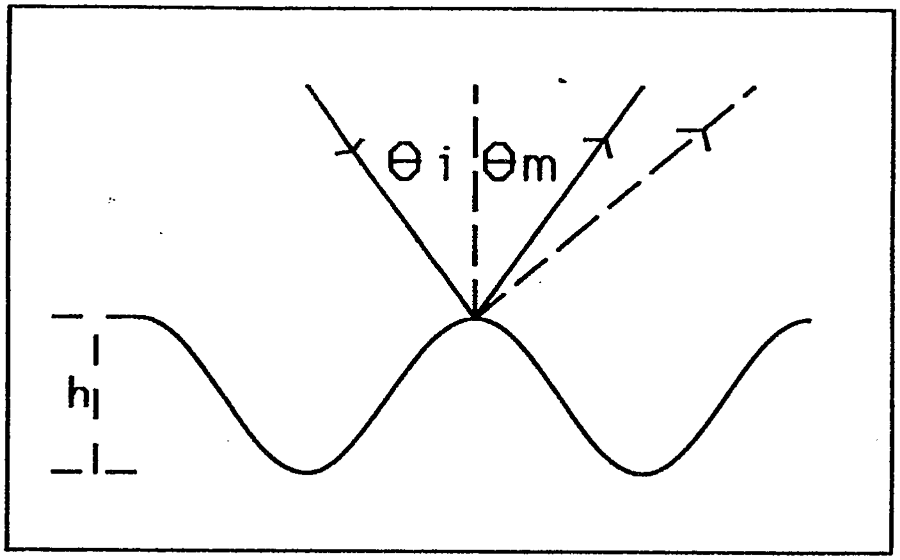

Fig. 2.1 The schematic of diffracted beam from an ideal sinusoidal surface.

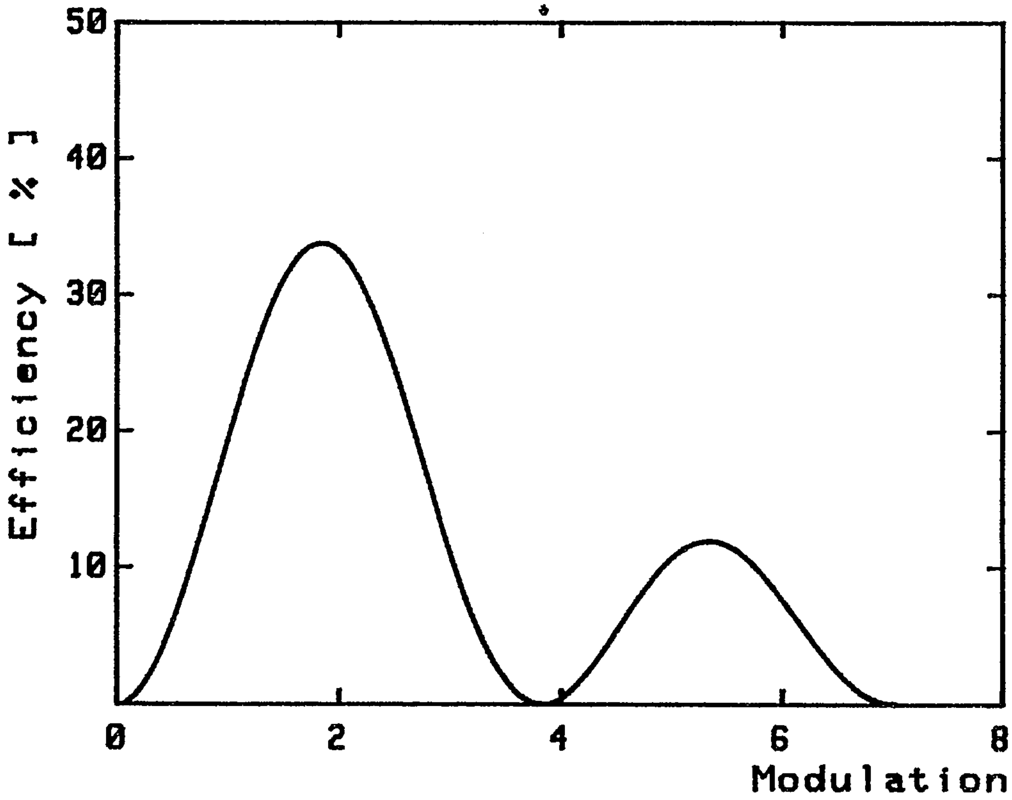

Fig. 2.2 Calculated diffracted efficiency for m = 1.

CHAPTER 3 THEORY

3.1 An Overview.

Several models have been suggested to explain the phenomena of the photo-induced electrochemical etching, where mostly the hole transport is the only consideration [3]. A simple but straightforward model has been proposed to explain the photo-induced electrochemical etching mechanisms [12].

Here, we are going to express the photo-induced electrochemical etching behaviors, starting with the photo-generated carriers reaction and ending with the removal of the dissolved species formation. The photo-generation of electron-hole carriers at the specimen may be considered as the absorption of the photon's energy and then the releasing of the carriers generated. Both the carriers transport and the removal of the dissolved species at the surface is modeled on the modified continuity equation which will be discussed in the next section. The model shows that the rate is proportional to the non-linearity of the coupling between the oxide formation and transportation of the oxides.

The exact mechanisms which govern the ionic flux through the oxide layer and the oxide thickness are not yet known. To simplify the problems, the model proposed is made of the following assumptions :

(1). We limit to a one dimensional problem normal to the specimen surface, thus the lateral diffusion is being ignored.

(2). The carriers are constantly generated and removed from the interaction region.

(3). The ionic current through the oxide barrier is dictated by the reaction rate.

3.2 Photo-Generated Holes.

In the photo-generated carrier's processes, the excitation due to the light is governed by the photon energy, $h\nu$. This should be greater than the energy band gap E_g of the bulk semiconductor InP. The optical excitation increases the electron and hole density above their equilibrium value. The photo-generated holes rate, G_p, at the specimen-electrolyte interface due to the two intersecting beams, is determined by the incident light intensity. The intensity of the spatial pattern here varies sinusoidally in the direction parallel to the specimen surface, i,e. in the direction of X-axis of the Fig. 3.1. Thus we write for the light intensity impinges on the specimen surface as follows :

$$I(x) = I_1 \left(1 + \cos \frac{2\pi x}{d} \right) \qquad < 3.2.1 >$$

Where holes are generated in a rate of G_p resulting from the absorption of the light, we write

$$G_p \propto \frac{\alpha\ I_1}{hv}\ exp\ (\ -\alpha\ y\ )\ (\ 1 + cos\ \frac{2\pi x}{d}\ ) \qquad < 3.2.2 >$$

Where α is the material absorption coefficient, I_1 is the average incident intensity at specimen surface $y = 0$, hv is the photon energy, d is the interference spacing which is given by the Bragg relationship with

$$d = \frac{\lambda_o}{2\ n_e\ sin\theta_1} \qquad < 3.2.3 >$$

λ_o is the free space optical wavelength, n_e is the electrolyte reflective index, and $2\theta_1$ is the incident angle. Under our model assumption, the generation carrier's rate and the removal from the interaction region is constant and linearly dependent on the laser intensity. The factor ($1 + \cos 2\pi x/d$) will image the sinusoidal variation (grating) patterns variation in the lateral direction. It is possible to reduce the grating's period by varying the incident beam's angle (for the fixed or given optical wavelength), using a shorter wavelength source or high-index prism [13]. Also, a shorter wavelength will have a larger absorption coefficient.

The absorption coefficient α will vary from the absorption coefficient for normal incidence, because the incident intensity results from the two beam of non-zero incidence angle. However, since the specimen has a high index reflective, this difference is of minor, consequence.

3.3 Electrolyte Diffusion Current.

It is understood that the carrier tends to move from a higher concentration region to a lower concentration region. The existent of the variation of the carriers concentration causes a process what we call *Diffusion.*

The basic driving force of the diffusion process is the electrolyte concentration gradient $\frac{\partial C}{\partial y}$. The flux F is proportional to the electrolyte concentration gradient, and the ionic atoms will be diffused from a high concentration region towards a lower one.

Let's consider the electrolyte-specimen interface distribution as shown in Fig.3.2, where the reactants diffuse through the interface layer and result in a concentration of $\bar{C}_o$ at the interface of InP specimen. The concentration gradient can be written as a proportional relation of

$$\frac{\partial C}{\partial y} = - \lambda_c \bar{C}_o \qquad < 3.3.1 >$$

where λ_c is the proportional constant, and $\bar{C}_o$ is the effective electrolyte concentration at the electrolyte/oxide interface.

3.4 Schottky Diode.

It has been known since 1938 that the diode arising from a potential barrier as a result of stable space charges in the semiconductor exhibits a rectifying behavior and is said to be a *Schottky Diode.*

Since the specimen is in contact with the electrolyte, both having a different fermi level and a stable barrier, so we may assume that the model arising is of a *Schottky Barrier.* In the Schottky Barrier, the current transport is mainly due to the majority carriers density. We associate the majority carriers density with the ionic species of the electrolyte concentration. Let us assume the surface work function of $q\phi_{es}$ between the electrolyte and the specimen surface. The holes at the specimen surface tend to flow into the electrolyte and there is an opposing balanced flow of a positive ion from the ionic electrolyte into the specimen surface. The interface carriers density p may be related as

$$\begin{aligned} p &= N_A \exp(-qV_{bi}/kT) \\ &= N_A \exp(-q(\phi_1 - V_n)/kT) \\ &= N_V \exp(-q\phi_1/kT) \end{aligned} \qquad < 3.4.1 >$$

Where ϕ_1 is surface work function (or ϕ_{es}) and is modeled [12] by using $\phi_1 = \Delta\mu C - V - \phi_2$. V is the external applied field, ϕ_2 is reduction in the surface potential due to image charge in both sides of the barrier, and $\Delta\mu$ is the chemical potential difference of active ions between the electrolyte and the specimen surface. Due to the incident photons and oxides layer built up, an oxide barrier of ϕ_3 is created. The ionic flux towards the semiconductor passes through this potential barrier formed by the oxides. The barrier is denoted by

$$\phi_3 = - \alpha_2 \, p \, C \qquad < 3.4.2 >$$

α_2 is a proportionality constant and C is the electrolyte-specimen interface concentration. Due to the photo-illumination on the specimen surface and the photo-voltage created, the surface electrolyte current J_c which follows the Schottky Diode is expressed in terms of

$$\begin{aligned} J_c &= J_o \, [\exp(q\phi_3/kT) - 1 \,] \\ &= J_o \, [\exp(-q\alpha_2 pC/kT) - 1 \,] \qquad < 3.4.3 > \end{aligned}$$

Where J_o is the saturation current density and is proportional to

$$J_o \propto N_v \exp\,(q\phi_1/kT)$$

3.5. Continuity Equation.

The photo beam introducing on the specimen surface gives rise to a coupling reaction between the electrolyte ionic species and the photo-generated carriers at the specimen interface with a rate of

$$R = \alpha_1 \, p \, C \qquad \langle\ 3.5.1\ \rangle$$

Where α_1, the surface coupling reaction proportionality, depends on the electrolyte composition and concentration, and incident laser source. p is the photo-generated carriers at the interface and is linearly proportional to the incident intensity, and C is the electrolyte concentration at the specimen interface.

The modified continuity equation on the electrolyte-specimen interface can be expressed in terms of diffusion and coupling reactivity by

$$\frac{\partial C}{\partial t} = \left(\frac{1}{q} \frac{\partial J_c}{\partial y} - R \right)(1 - \rho)$$

$$= \left(\frac{1}{q} \frac{\partial J_c}{\partial y} - \alpha_1 \, P \, C \right)(1 - \rho) \qquad \langle\ 3.5.2\ \rangle$$

Where $(1 - \rho)$ is the surface state and is written as $(1 - \rho) = 1/[\exp(-\phi_1/\phi_Q) + 1]$ with $\phi_Q = kT/q = 0.026$ V at the room temperature, and ϕ_1 is the surface potential.

Now, if we substitute J_c from equation < 3.4.3 >, the above equation < 3.5.2 > becomes

$$\frac{\partial C}{\partial t} = \left(\frac{\alpha_2 \, J_o}{k \, T} \, p \, \frac{\partial C}{\partial y} \exp(-q\alpha_2 pC/kT) - \alpha_1 \, p \, C \right)(1 - \rho)$$

$$= \left(\frac{\alpha_2 \; J_o \; \lambda_c}{k \; T} \bar{C}_o \; p \; \exp(-q\alpha_2 pC/kT) \; - \; \alpha_1 \; p \; C\right)\left(1 - \rho \right)$$

$$= \left(\beta \; \bar{C}_o \; p \; \exp\;(-\alpha_o pC) \; - \; \alpha_1 \; p \; C \right)\left(1 - \rho \right) \qquad < 3.5.3 >$$

$\beta = (\alpha_2 \lambda_c J_o)/(k\ T)$ is the effective diffusitive coefficient and α_o is $(q\ \alpha_2)/\ kT$. For the system suggested, the $\bar{C}_o$ acts as the ionic current source. For the reservoir system we may solve the non-zero steady state electrolyte concentration($\frac{\partial}{\partial t} = 0$) with a relationship between the steady state electrolyte concentration C_{ss}, the reactivity α_1, and the effective diffusion coefficient β, as

$$C_{ss} = \frac{\beta}{\alpha_1} \bar{C}_o \; \exp(-\alpha_o p_s \bar{C}_o) \qquad < 3.5.4 >$$

The etching/reaction rate $R=C_1\alpha_1 p_s C_{ss}(1-\rho)$ can be evaluated for steady state condition, (reservoir system) as

$$R = C_1 \; \beta \; p_s \; (1-\rho) \; \bar{C}_o \; \exp(-\alpha_o p_s \bar{C}_o) \qquad < 3.5.5 >$$

Where C_1 is the reaction proportional constant. We may assume from the equation < 3.5.5 > that the rate R is proportional to the minimum reaction time T

$$R = \frac{(1 - \gamma \; C_o)}{T}$$

Where γ is a non-negative constant less than unity. The relation between the reaction time and the electrolyte concentration $\bar{C}o$ can be illustrated as in the Fig. 3.4 shown (see page 28).

For a closed system (capillary film), one may solve the steady state eq. < 3.5.3 > by approximating the surface electrolyte concentration $\bar{C}_o$ to the steady state concentration C_{ss}, thus $C_{ss} \approx \bar{C}_o$. The equation < 3.5.4 > becomes

$$C_{ss} = \frac{-1}{p_s \ \alpha_o} \ln(\alpha_1/\beta) \qquad < 3.5.6 >$$

And the reaction rate R becomes

$$R = - \frac{C_1 \ \alpha_1}{\alpha_o} (1-\rho) \ \ln \ (\alpha_1/\beta) \qquad < 3.5.7 >$$

with the rate R is explicitly independent of the incident intensity.

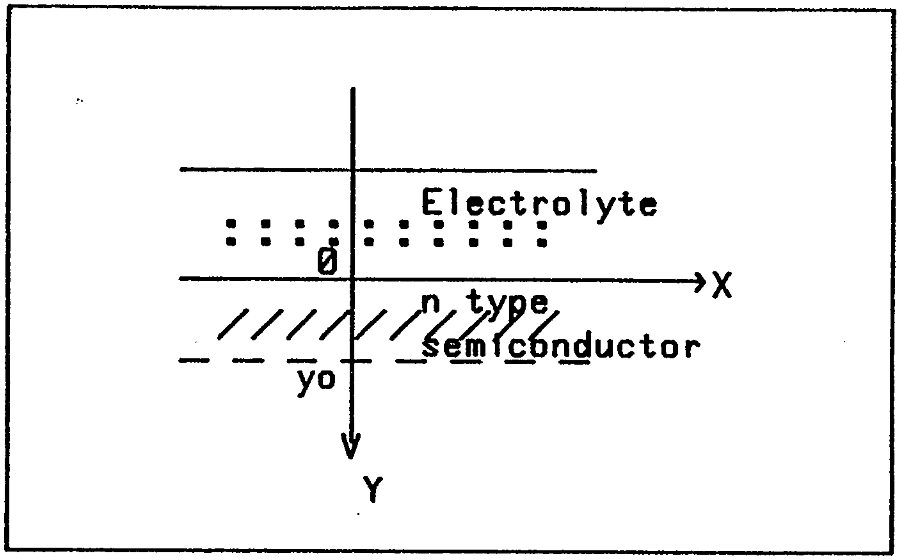

Fig. 3.1 Diagram of the specimen- Electrolyte interface.

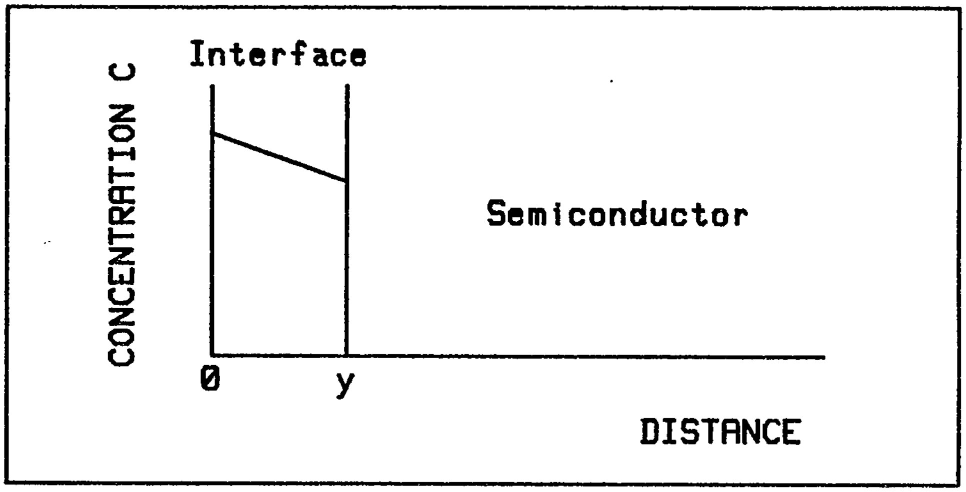

Fig. 3.2 The basic electrolyte layer characteristics at the interface.

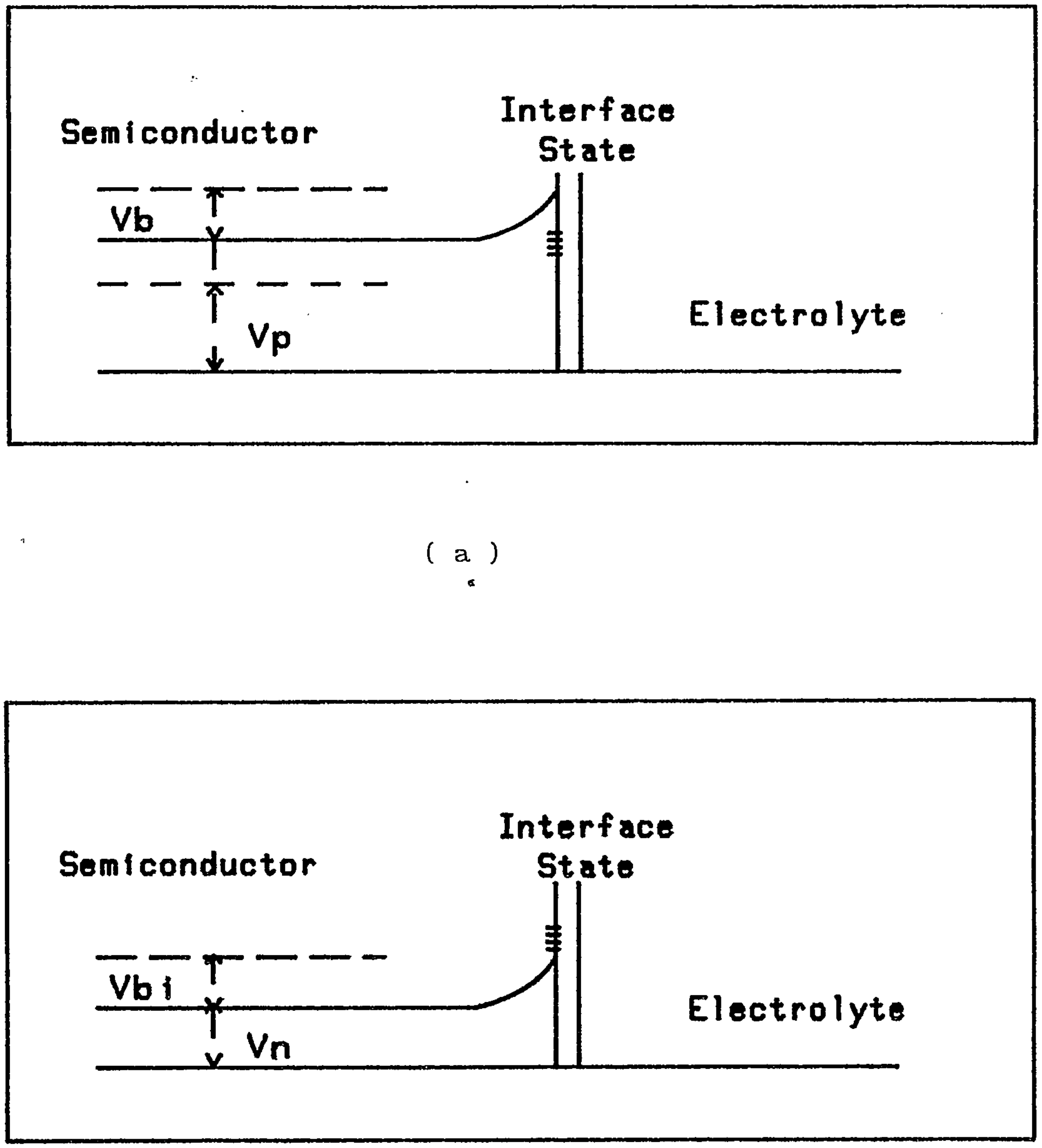

(a)

(b)

Fig. 3.3 Diagram of interface showing band bending, energy level (a) equilibrium (b) under illumination. V_p owing to the photo-induced potential.

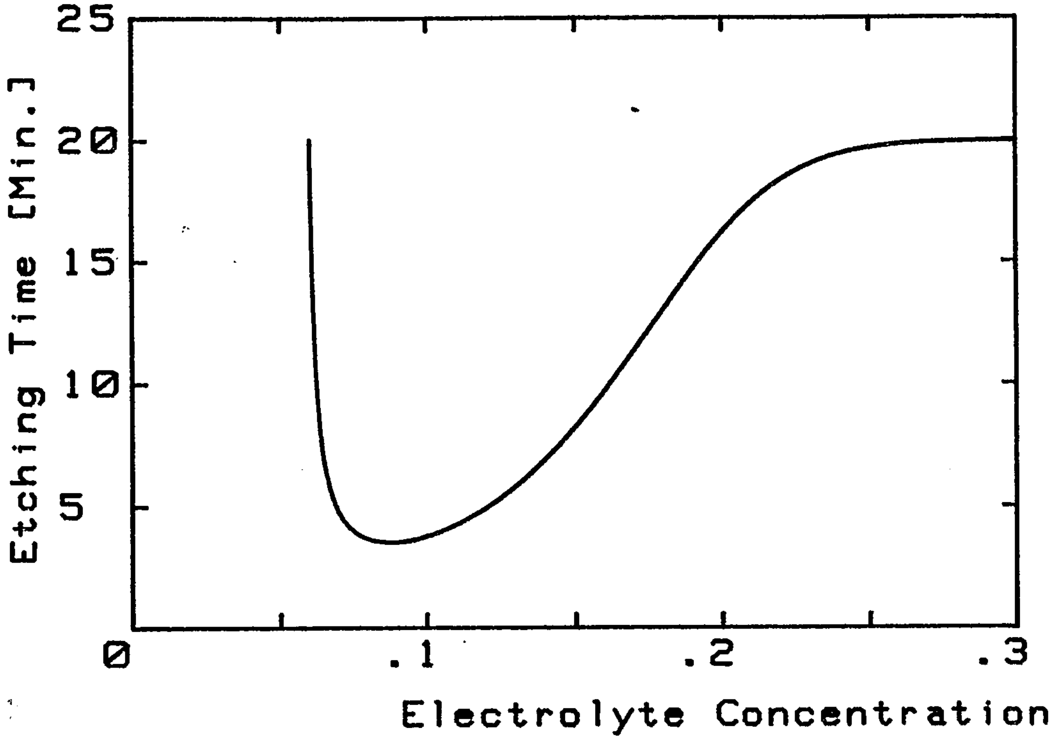

Fig. 3.4 The electrolyte concentration effect on etching time.

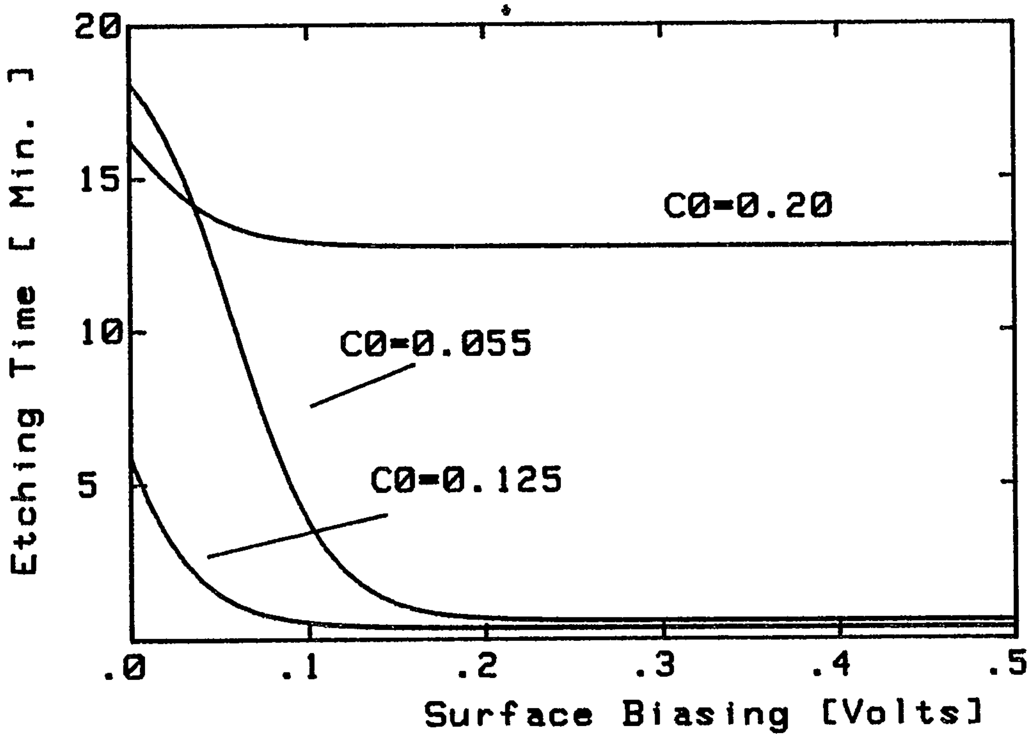

Fig. 3.5 External biasing field effect on etching time for various concentration C_0 (a) .055 (b) .125 (c) .2

CHAPTER 4 EXPERIMENTS

4.1 Apparatus Set-up.

Since a high-resolution grating patterns is achieved by interfering the two laser beams, care must be taken to insure that the optical path length of each laser beam arm is approximately equal and the optical table is acoustically isolated. Any optical disturbances of the etching beam should be avoided.

The scheme of the interferometric arrangement used to produce the grating patterns is shown in Fig. 4.1. The light from the laser source of He-Cd of wavelength λ = 442nm is split into two beams of nearly equal intensity by means of an half mirror, then intersecting on the InP wafer surface, at an angle of $2\theta_i$. The wafer is sprayed with a small quantity of electrolyte solution which spreads in a thin film by the capillary action under a cover glass. The full mirrors used for reflection purposes are of reflectivity of 99 %. Thus, interference fringes will result in a sinusoidal intensity variation as given in Eq.< 3.2.1 >

The glossary description of Fig. 4.1 (see p 41) is given below:

1. *UV Laser* - Optical source, wavelength λ = 442 nm.

2. *Beam Splitter (Half Mirror)* - Splitting the optical source into two nearly equal in intensity beams.
3. *Mirror (M1, M2, M3)* - Full reflectivity mirror. To bring the beam into the intersecting point.
4. *Laser* - Second laser source. To detect the grating formation. Low photon energy is preferred.
5. *Lock-in amplifier* - To analyze the diffracted beam intensity of gratings formation at the sample surface. It reduces noise to minimum. The reference frequency is provided by the optical chopper.
6. *Optical chopper* - To provide a reference frequency to the lock-in amplifier.
7. *Detector* - Photodetector, to detect the beam intensity and send the signal to lock-in amplifier.
8. *Lenses* - Optional. Used to adjust the incident beam diameter and intensity.

The incident laser intensity was detected by using a UV photodetector (EG & G, UV - 100BQ), and was measured as approximately 0.10 [W/mm^2] per beam at the specimen surface. A second laser source was used for grating diffraction monitoring. This monitoring laser is of low power. A He-Ne laser with a wavelength of $\lambda = 0.6328\ \mu m$ was being used here. The diffraction pattern of this laser is recorded at the Fourier plane of the lens imaging the semiconductor surface.

4.2 Material Preparation.

The significance of the surface contamination and cleaning before etching are closely associated with the practical etching process. Surface contaminations can be considered in two ways : initially present contaminants prior to etching, and residual contaminants arising after the etching process.

The contaminations on the surface prior to etching may consist of particulate materials. A simple mechanical means is polishing, then rinsing in wet cleaning, preferably by distilled water; de-ionized distilled water is recommended to avoid recontamination of the surface.

4.2.1 Specimen Surface Cleaning and Polishing.

The contaminations on the specimen surface prior to etching should be removed since they may interfere with the etching by undesirable reactions with the electrolyte/etchant. There are several ways of removing these particulates, such as ultrasonic treatments in cleaning solutions, use of compressed gas jets, chemical - mechanical polishing, etc. [14].

For our experiment here, a simple chemical - mechanical polishing is used to give an optical flat and damage-free surface. The bromine-methanol (Br_2-CH_2OH) with aluminium oxide (Al_2O_3) is selected to clean and polish the specimen surface. First, the mechanical polishing is done by using the Al_2O_3 powder (with particle size of .06 µm), then the chemical polishing with bromine-methanol solution follows. The specimen is dipped in the freshly prepared bromine-methanol solution for about 90 sec., then rinsed with the distilled, deionized water. (we propose after that to dry it out in N_2 gas blow). In this way, we hope to minimize the unintentional oxidation on the surface. The oxide layer was measured by using *ellipsometer, type 43603-200E*, and it was found that the oxide layer can be polished up to approximately 100 Å. More than one type of oxides may exist. However, the major type is In_2O_3 for this n-InP, < 100 > orientation specimen. [8].

4.2.2 Electrolyte Solution.

There are many electrolyte solutions that have been experimentally used for the surface dissolution of n-InP, such as $H_2SO_4/H_2O_2/H_2O$; H_2SO_4/H_2O; 2M HCl; $HCl/HNO_3/H_2O$, etc. [15].

In order to get the smoothest etched surface and deepest triangular profiles on < 100 > InP specimen surface, the 37 % HCl / .996N HNO_3 / H_2O aqueous electrolyte solution is used with relatively small HNO_3 concentration [3]. The relative volume concentration being used here is of HCl : HNO_3 : H_2O is 1 : 3 : X, where X is aqueous dilution parameter.

4.3 Experimental Procedure.

The characteristics and microscopic behaviors of the photo-induced electrochemical etching on the semiconductor surface is carried out through the experimental below.

After the InP specimen has been cleaned and polished as described in sec. 4.2.1, a small quantity ($\approx 1.5 \times 10^{-6}$ l) of the electrolyte solution of the specified concentration is dropped on the specimen surface by using the neutralization pipet. Then a cover glass is put on the specimen. By the capillary effect, the electrolyte solution is spread uniformly over the specimen surface. This prepared specimen can start the photo-induced electrochemical etching process by putting it under the intersecting beams shown in the Fig. 4.1.

A single focal lens is used to focus the beams intersecting on the specimen surface. The spot size is approximately at the focal point or any point according to the spot size of interest. During the experiments the spot size is fixed without varying the experimental parameters.

4.3.1 Electrodeless Process.

The electrodeless process is an interesting and important phenomena in the photo-induced electrochemical etching process. It is done with no external potential being applied to the specimen. The process is done directly after the specimen has been prepared as described in section 4.2. Most of the processes carried out in these experiments are of electrodeless process except that of sec.4.3.5. The electrodeless schematic is shown as the Fig.4.2.

The procedure steps are carried out as following :

1. Chemical polishing and cleaning the specimen with Br_2-CH_2OH or mechanical polishing with Al_2O_3 then chemical polishing with Br_2-CH_2OH.
2. Rinse with distilled water.
3. Drop a small quantity of the specified concentration electrolyte over the specimen.
4. Put on the cover glass.
5. Etch under the illumination of the intersecting He-Cd laser beam. Record the etching time needed.
6. Clean with distilled water, and observe under the microscope. Record the minimum etching time.

The etching time is defined here as the minimum exposure time needed in order to get a measurable etching grating.

4.3.2 Electrolyte concentration Effect.

To understand the effect of the electrolyte concentration with reference to the etching time, we are proceeding to the experiments as described in section 4.3.1 for different electrolyte concentration by changing the water dilution parameter X from 6 to 50.

Since it was stated that the photo-generated holes at the interface induce the formation of the oxide which in turn may affect the etching time, therefore we compared the process results from polished and non-polished surfaces.

Polishing process is a process in which the specimen has to be cleaned and polished as the steps 1 & 2 of section 4.3.1 after the etching is completed. For example, the process follows step 1 through 5 of section 4.3.1 , then clean the specimen as step 1 & 2 before the next electrolyte concentration (or other parameter) etching process takes place. The non-polishing process is a process in which the etching is done thoroughly without cleaning and polishing the specimen, but in which the specimen is just rinsed with the distilled water. Then the next electrolyte concentration etching follows, i.e. omitting the step 1 & 2 of section 4.3.1.

4.3.3 Electrolyte Layer Characteristic Effects.

It is known that the photo-induced electrochemical etching of the semiconductor surface proceeds by the transportation of the reaction to the specimen surface, i.e by diffusion. The diffusion of the ionic electrolyte into the reacting surface is affected by the electrolyte -specimen thickness, which in turn acts as the reactants' source.

Hereby we attempt to carry out the etching process experimentally by adding certain weight on the cover glass such as that affecting the electrolyte-specimen interface layer thickness . The schematic configuration is shown in the Fig. 4.3, where the weights on the cover glass are of 1 gr (cover glass only), 4.6 gr, 8.0 gr, and 39.5 gr. The estimated electrolyte layer characteristic thickness is 46 μm, 24.2 μm, 16.7 μm, and 7.4 μm respectively.

The experiment procedure is the same as the section 4.3.2 polishing process, except for adding the weight on the cover glass before etching process started.

4.3.4 Incident Laser Power Effect.

Let us now consider the effect of the incident laser intensity on the photo-induced electrochemical etching process. Instead of changing the electrolyte concentration, we keep the concentration fixed at $HCl/HNO_3/H_2O$ as 1 : 3 : 30 throughout the experiment.

The same laser source is being used as before. However, a multi-layered transparency is put in between the laser output beam and the specimen in such a way that the number of transparency layers are varyied in order to get the various of the incident laser intensity. The incident intensity being used in the experiment here is approximately 5, 10, 15, 30 [W/Cm^2]. The experimental steps are :

1. Put on a number of transparency.

2. Follow the step 1 to 6 of sec. 4.3.1 for the specified incident intensity. Record the etching time.
3. Clean and polish the specimen.
4. Change the number of the transparency layers, back to step 2.

4.3.5 Electrode Etching Process.

The following experiment explores the effect of the electric potential on the etching time. *The field effect experiment is a means* of varying the surface potential without changing the ambient. By a capacitively applied external electric field normal to the surface, the surface conductance of the specimen is varied [16]. The schematic configuration of the applied potential on the specimen is shown in the Fig. 4.4.

It is known that the interface of the electrolyte and the specimen surface forms a potential barrier. By introducing the external biasing field, we are expecting to increase the total of induced holes on the specimen surface per unit area where they consist of the space charge region and surface state charges; and the potential barrier is lowered by the effect. The cathode electrode is applied at the electrolyte and specimen surface, and the anode at the bottom of the specimen. By means of acid ionization, the cathode electrode would be uniformly distributed throughout the specimen surface. An adjustable voltage source is used, and the electrolyte concentration being used during the experimental is kept constant.

The experimental steps are following,

1. Polish and clean the specimen as section 4.3.1, step 1 to 3.
2. Put the anode in the bottom of the specimen.
3. Put the cathode at the specimen surface. Keep it in contact with the electrolyte solution.
4. Adjust the voltage source to the specified value and record it.
5. Then put on the cover glass. Take advantage of the capillary effect and *acid ionization*, so that the field is uniformly distributed in an upward direction.
6. Start to etch. Record the etching time.
7. Clean with distilled water, and polish the specimen before go on the next potential value.

4.4 Grating Growth Measurement.

The growth of the grating depth with the time may be observed by monitoring the diffracted beam intensity, either zero or ± first order diffracted beam. The beam diffracted due to the grating growth was detected by the photo-detector.

The first order diffracted beam is weak, due to much of scattering and diffusion losses, thus an optical chopper which provides a reference frequency to the lock in amplifier as shown in the Fig. 4.1 is used to increase the signal to noise ratio. The laser source is modulated using the optical chopper and is detected by the detector. The signal, including the background noise from the detector was sent to the lock-in amplifier. By comparing the signal from the detector to the reference frequency of the optical chopper, the background noise which does not pass through the optical chopper is reduced to a minimum level.

The frequency of the optical chopper is chosen not to be near the power system frequency, e.i 60 Hz or its integer multiplication, to avoid the line noise. In the experiments a 150 Hz frequency was used.

4.5 Experimental Results.

In the experiments above, we have measured several effects that related to the photo-induced electrochemical etching process. The results show out a good agreement with the model as expected.

The experimental results depicted in the figure shown are carried out in the procedure described in the previous section. The etching time for polished and non-polished process as a function of electrolyte concentration is carried out as described in the experimental procedure section 4.3.2. The etching time for each electrolyte parameter is ascertained by etching several definite etching time, and the minimum etching time is observed under an optical microscope. The process is repeated to minimize the errors that may occur. The results are given in the figure 4.5. The figure 4.6, where the experimental is done according to procedure section 4.3.3 , reveals the effect of incident laser intensity on the etching time for various electrolyte layer thicknesses. We may conclude that the holes' density is linearly dependent on the incident laser power [17,18] (see also the experimental result figure 4.6(d)). And figure 4.7 where the experimental is done according to procedure section 4.3.4 gives the effect of intensity to the etching time for the relative electrolyte content of 1:3:30. The external biasing effect is described in the procedure section 4.3.5, and results in the etching process being enhanced, especially for a low electrolyte concentration. This is shown in the figure 4.8 and 4.9. The etching rate is being monitored by detecting both the first order diffracted intensity beam and the zero order diffracted intensity beam. The results of these are shown in the figure 4.10 and 4.11.

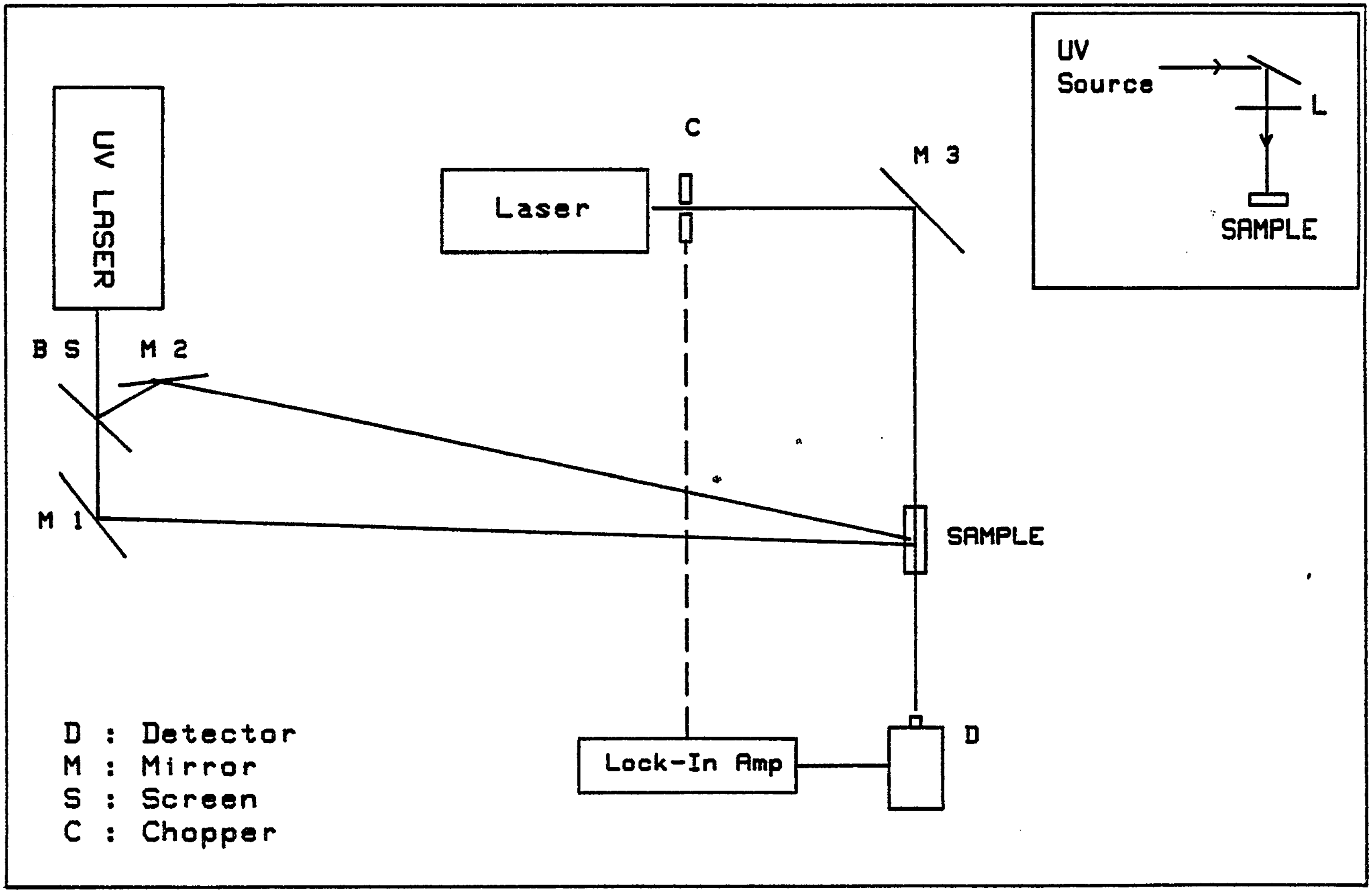

Fig. 4.1 Experiment Schematic

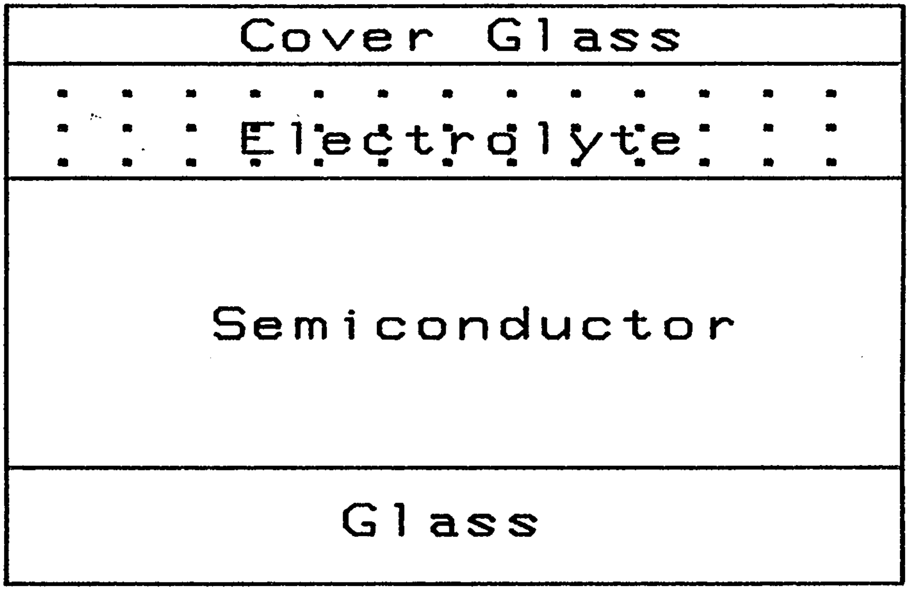

Fig 4.2 Electrodeless specimen etching configuration.

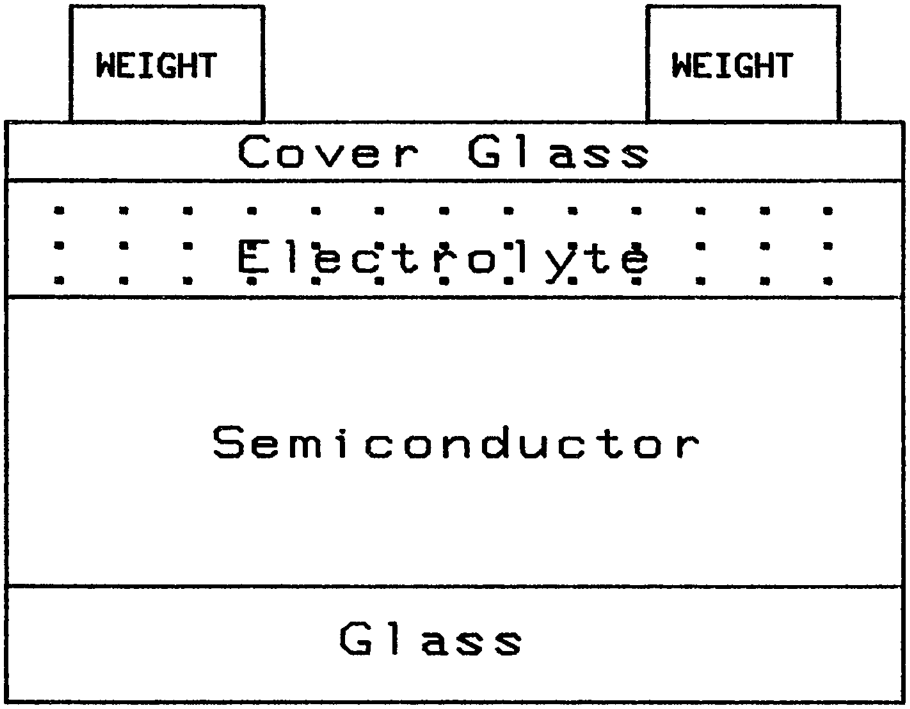

Fig. 4.3 Electrolyte layer control schematic

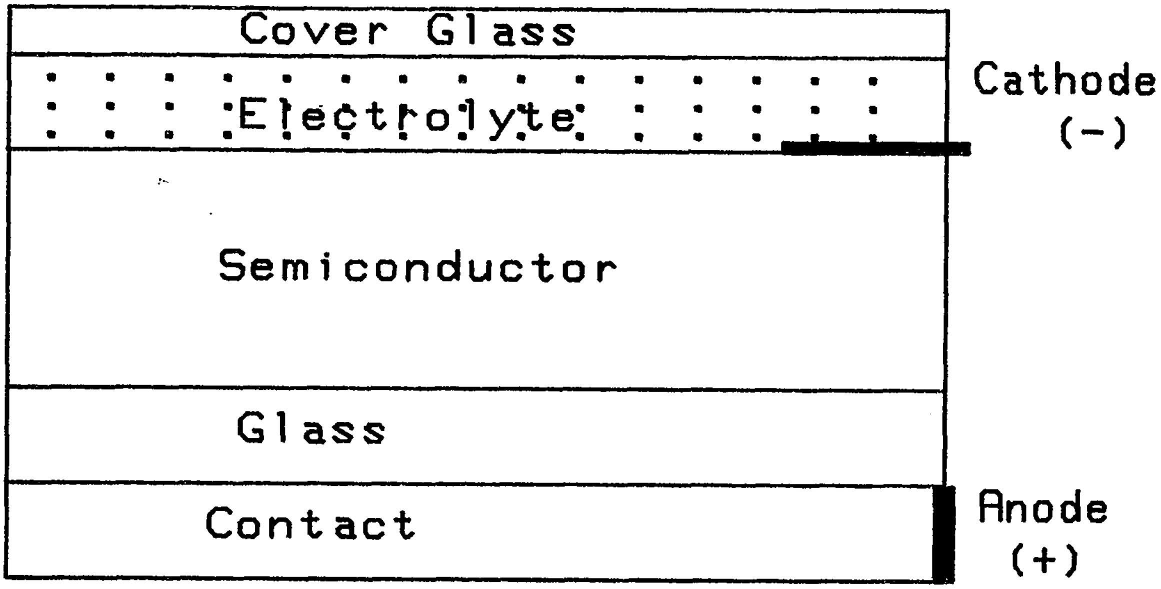

Fig. 4.4 The External electric-field configuration.

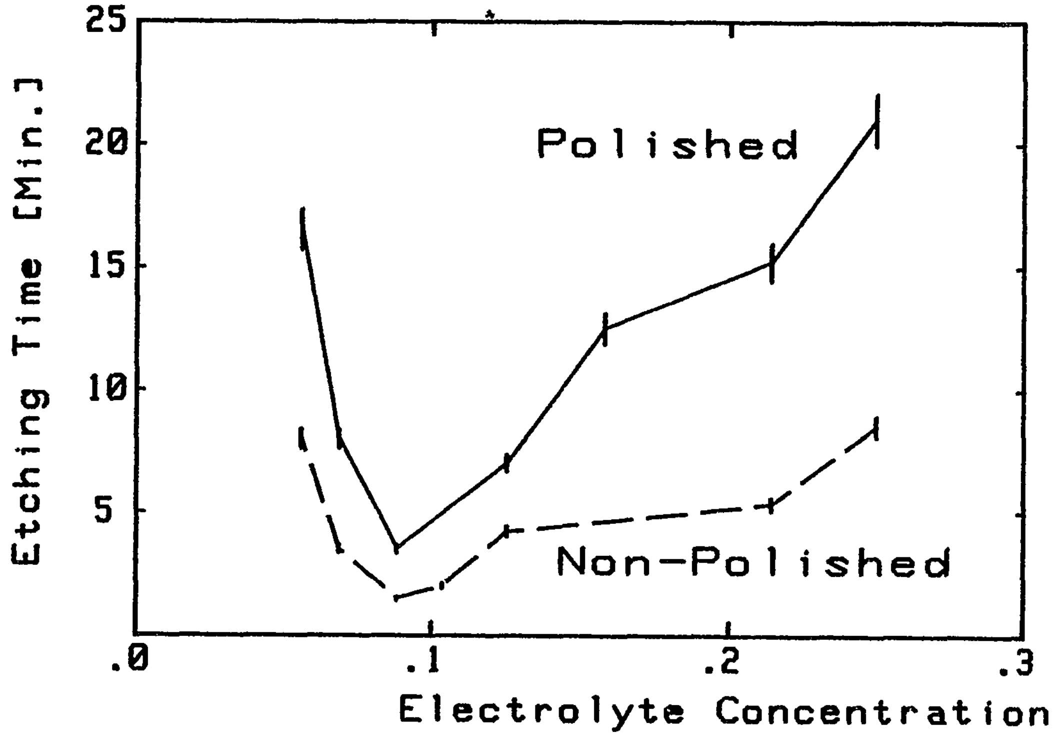

Fig. 4.5 Effect of Electrolyte Concentration to Etching Time for

(a) Polished; (b) Non-Polished conditions.

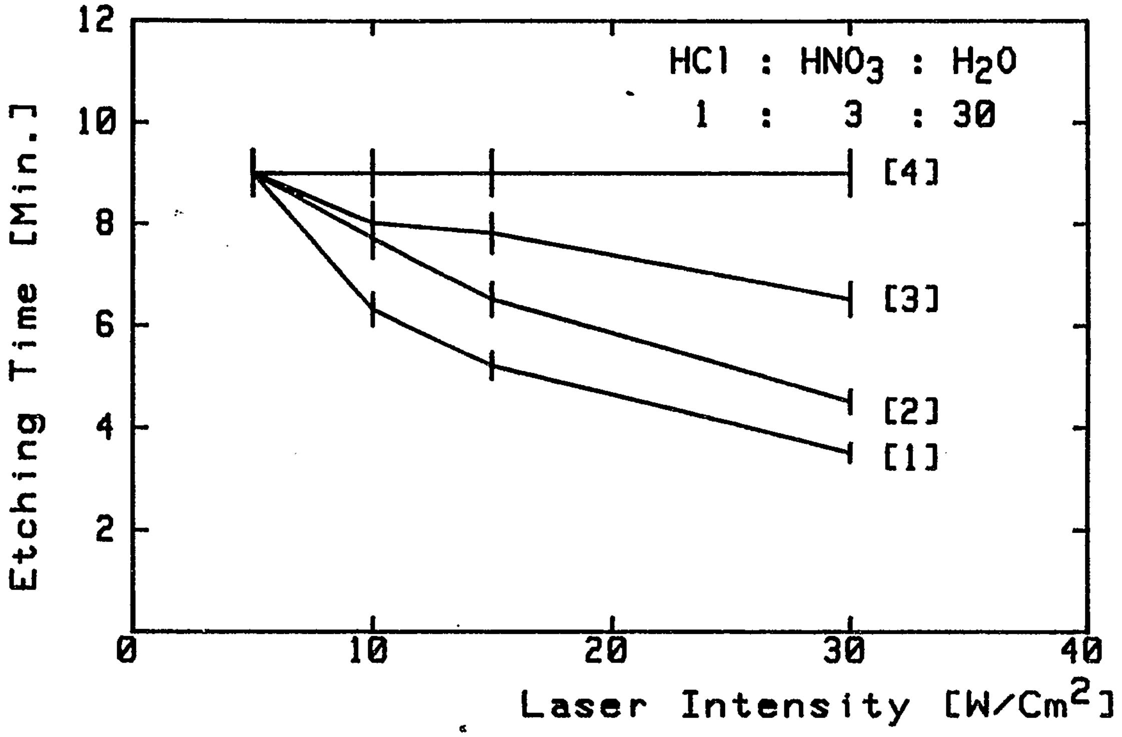

Fig. 4.6 Effect of the Electrolyte Layer Thickness to the Etching Time for (1) 46 (2) 24 (3) 17 (4) 7 μm thickness.

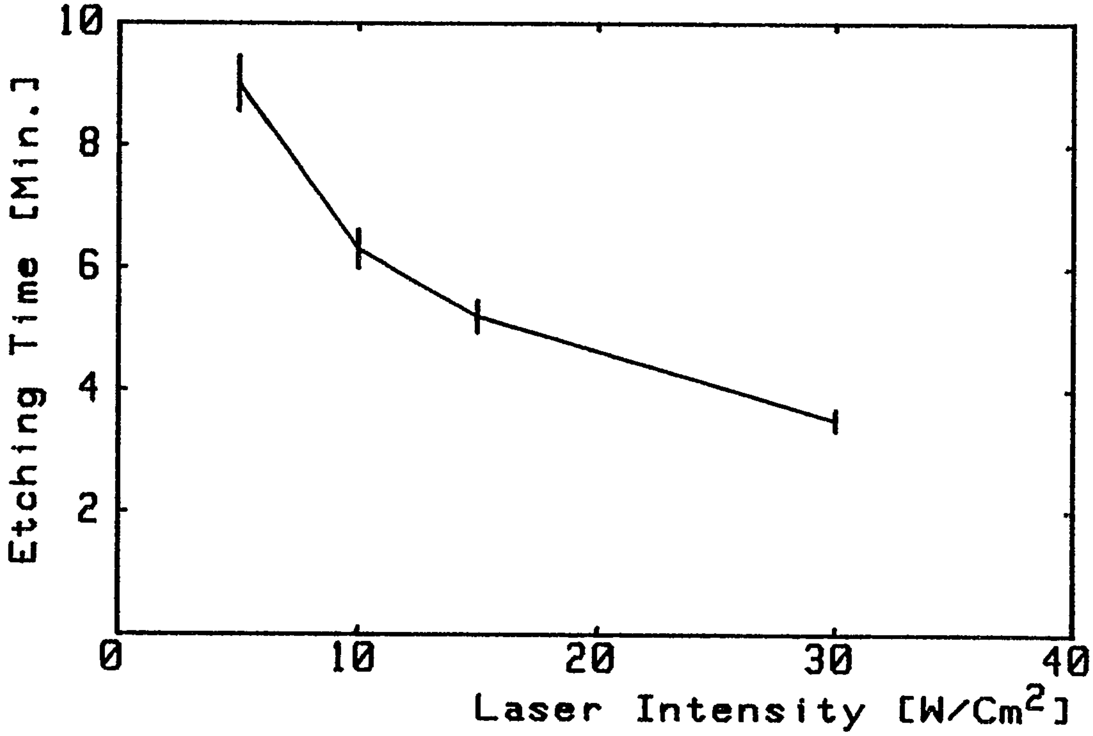

Fig. 4.7 The Laser Intensity Effect on the Etching Time

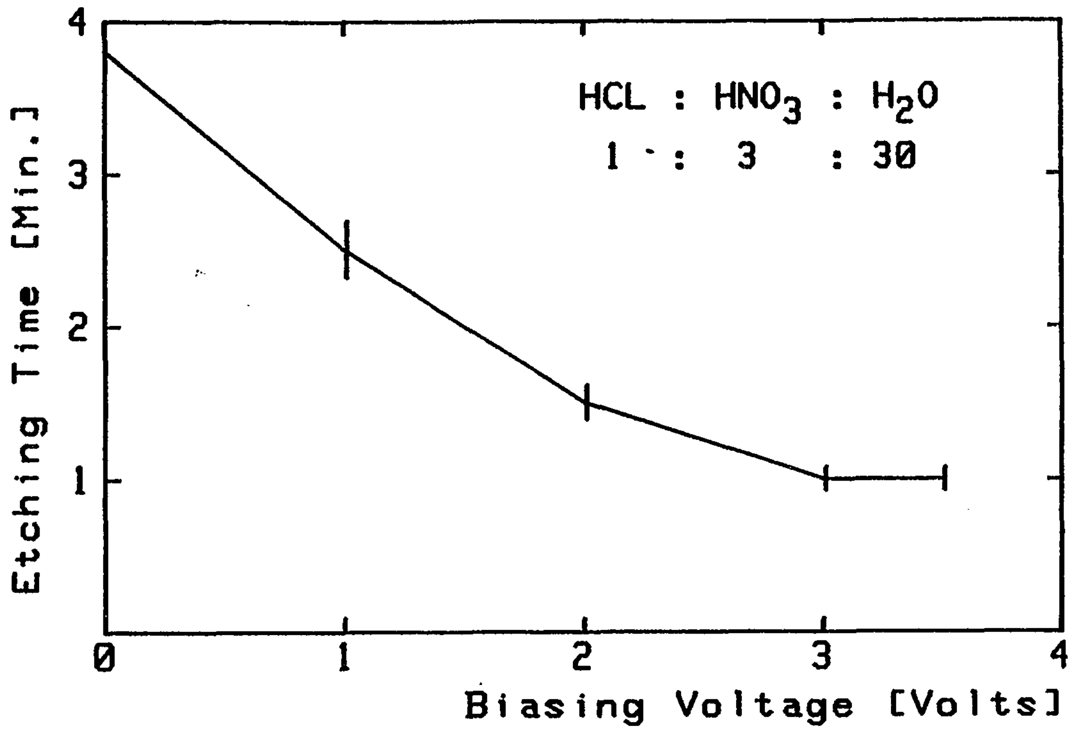

Fig. 4.8 The External Biasing Effect on the Etching Time

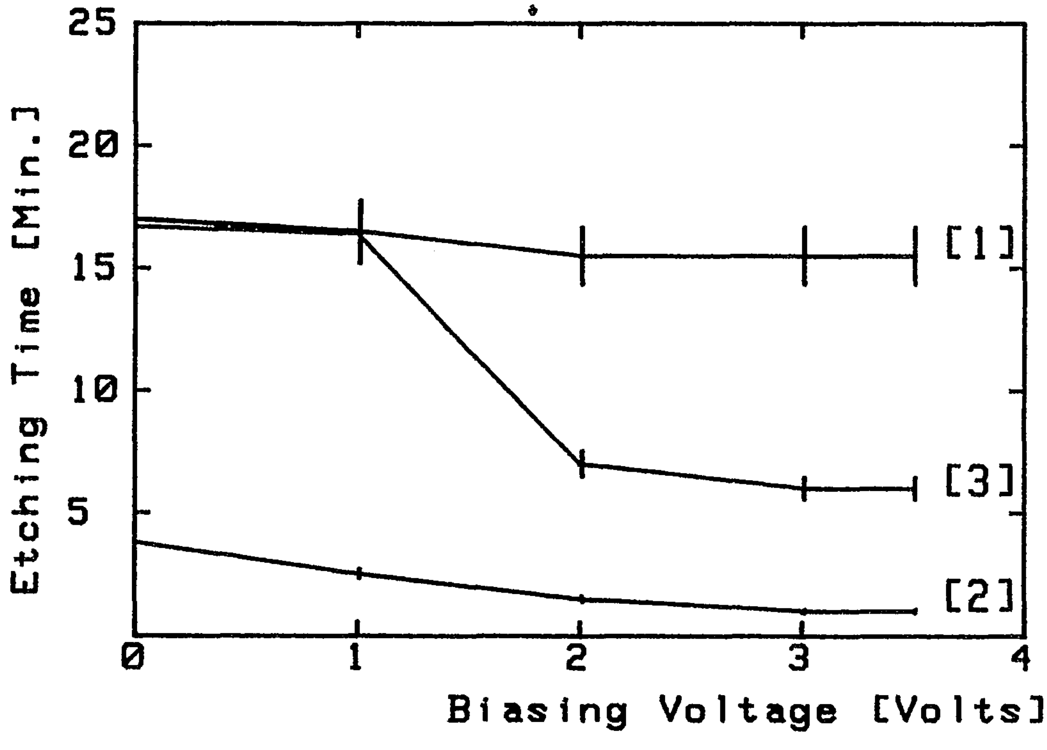

Fig. 4.9 The External Field Effect on Etching Time for HCl:HNO3:H2O

(1) 1:3:10 (2) 1:3:30 (3) 1:3:50 relative concentration

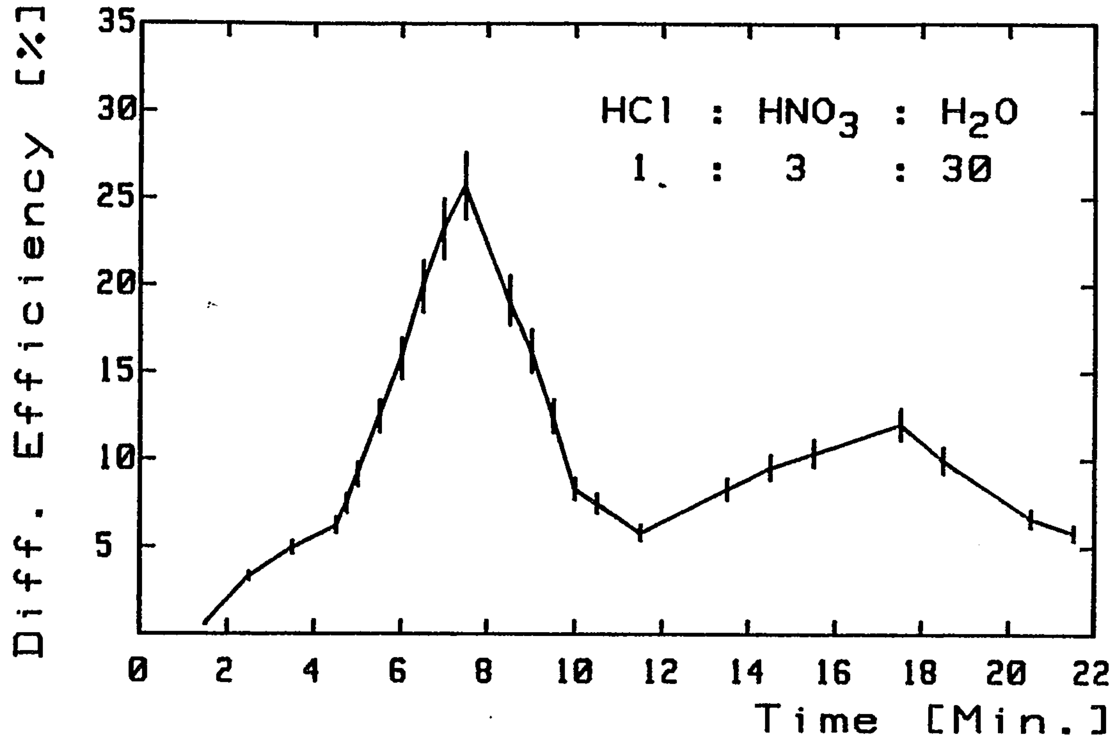

Fig. 4.10 Measurement first order Diffracted Efficiency for 10μm Grating in n-InP

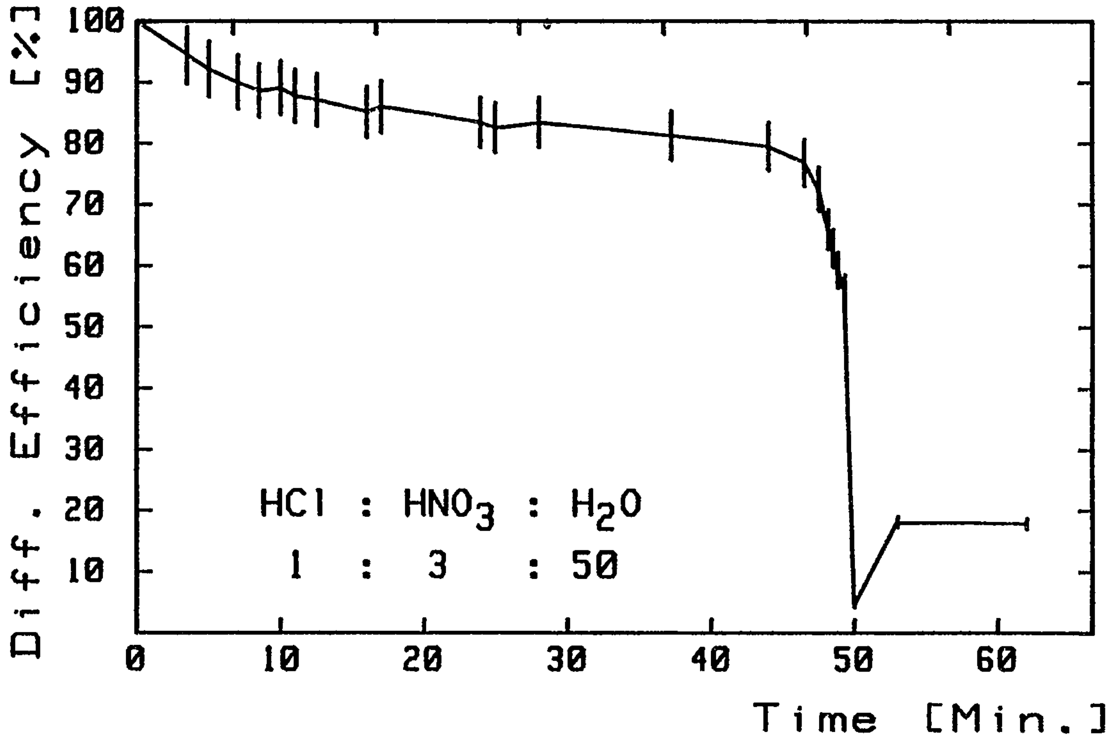

Fig. 4.11 Measurement Zero order Diffracted Efficiency for 10μm Grating in n-InP

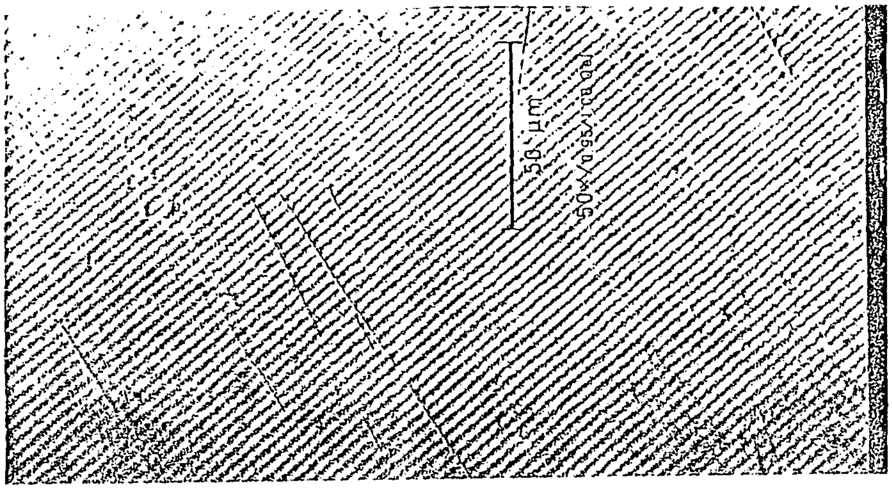

Fig. 4.12 The 2 µm grating patterns engraved on n-InP by photo-induced electrochemical etching.

CHAPTER 5 DISCUSSION

5.1 Grating Formation.

Since we attempt to image a sinusoidal grating pattern on the specimen surface, we have to assure that the two intersect beams are really intersecting on the specimen surface for the system used, so that the grating patterns may be engraved on the specimen surface. If the system is not well aligned, the patterns formed become non-sinusoidal patterns.

We have ignored the lateral diffusion contribution to the reaction rate, and also have only considered the one-dimensional continuity problem. Indeed, the lateral diffusion may be considered the surface recombinations since it may disturb the reaction rate. The effect becomes clear for a slower reaction rate concentration. The system is also sensitive to environmental conditions, i.e vibrations. In order to achieve an optical quality of smooth and well-defined sinusoidal grating, the system has to be isolated, vibration free, and the two intersecting beams of 90 degree incidence on the specimen surface. The tilt of the specimen causes a non-perpendicular incident angle illuminating the specimen, and consequently, changes the patterns engraved.

A monitoring second laser source is used to detect the image of the pattern. By introducing a uniform beam over the whole patterned surface, one can minimize the effect of the monitoring laser on the etched pattern. Also the second laser source selected is to be a very low of the photon power ($h\nu < E_g$) in order to neglect the disturbances to the minimum level.

5.2 Cutoff Spatial Frequency

It is also observed through the measurements of the exposure characteristics that there is a cutoff spatial frequency for the grating produced by this technique. At a high spatial frequency the modulation amplitude decreases rapidly. The cutoff spatial frequency is found to be about 2000 [mm^{-1}].

As the incident angle is increased, i.e the spatial frequency is increased, we find out that the etching rate decreases, as well as the modulation depth. These phenomena also have been studied previously [15]. Since the photo-induced electrochemical etching may be considered to be an imaging or projection system (either coherent, partially coherent or incoherent), thus the system (contrast or modulation) has a limited spatial frequency response [19]. The factors that limit this phenomena may have linear or non-linear properties, i.e scattering light during exposure and reaction diffusion, etc.

5.3 Discussion on the experimental results.

5.3.1 Change of the electrolyte concentration.

The experimental results of Fig.4.5 exhibit the non-linear relation between the electrolyte concentration and the etching time for both polished and non-polished processes. The optimal reaction rate for both etching processes occur at the same electrolyte concentration parameter. The results agree consistently with the model expected as given in the Fig. 3.4.

The right shift of the experimental results was explained as the result of the lateral diffusion and/or dark current contributions which were neglected in the theory considerations. It is understood that the experimental electrolyte concentration C_o is higher than that of the ionic current supplier concentration $\bar{C}_o$ and both these are more than the steady state concentration which took place in the surface reaction C_{ss}. One may empirically figure out the $\bar{C}_o \longrightarrow C_o - 0.05$, and this parameter contributes to the right shift of the Fig.4.5.

It is also observed from the experiments that at a higher HCl and lower HNO_3 concentrations (namely HCl : HNO_3 : H_2O = 1 : 1 : X) will give an optimal etching rate but increases lateral etching. With a relative low of HNO_3 content, one may get a deepest etching profile.

5.3.2 Electrolyte layer variation

The experimental results showing in Fig. 4.6 bring out that the photo-generated carriers density is linearly dependent on the incident laser power [18]. The reaction rate is the holes' density dependent as the reservoir system and explicitly independent of the incident laser intensity for capillary system. This also results in the expected model given in equation < 3.5.7 >.

we have mentioned previously that for the capillary system, the steady state electrolyte concentration is $C_{ss} \cong \bar{C}_o$. Under this assumption the reaction rate $\mathcal{R}$ becomes explicitly independent of the photo-generation holes density.

5.3.3 Change of Intensity

The change of photo incident intensity I_i may induce the change of carriers' generation which involves the surface reaction as seen in the equation < 3.2.3 > where $p = \tau_p G_p$.

For a low incident power the p creation is linearly proportional to the incident power. As the incident power increased to a certain value, the p created will reach the saturation value. This is shown by Fig.4.7 where the etching time is monotonously decreasing at the lower power and starting a steady etching time as the power is increased.

5.3.4 Change of the External Field

The experimental results in Fig. 4.8 reveal the correlation with the model predicted in Fig. 3.5. The external biasing field enhances the reaction rate for a low electrolyte concentration, the surface state described by ($1-\rho$) contributes much more to the lower concentration than to a higher one. When the applied field is increased, the surface state may reach its saturation level and not effect the etching time, relatively.

In the Fig. 4.8. the measurements are taken for various electrolyte concentrations for various values of the applied field. We can see that the applied field starts to reveal the enhancement effect after the field has overcome a certain barrier value.

5.3.5 Diffraction Efficiency

The sinusoidal grating depth formation is monitored through the first order diffracted efficiency. It is known that for a pure sinusoidal surface the diffracted efficiency is the Bessel function. The results shown in Fig.4.10 and 4.11 indicate the Bessel function but with minor differences,

1. The intensity resulted does not come to zero time abscissa.
2. The maximum first order diffracted efficiency does not reach the Bessel climax point.

These differences were explained as the results of (1) the sensitivity of the detector used and (2) the noise and the scattering due to the system surface in which not all diffracted beams went directed into the detector, etc.

CHAPTER 6 CONCLUSION

We have introduced the simple and straightforward model to control the photo-induced electrochemical etching on the III-V semiconductor (n-InP). The experimental results confirm to the model proposed. The technique is a suitable method for a direct fabricating of a deep profile but one in submicrometer range of a pure substrate.

The dependence on the surface reaction process at a low incident power and temperature is inconsistent with a thermal process, rather then the creation of hole-electron pairs by photo-irradiation. The reaction rate exists in a non-linear relationship between the electrolyte concentration and the induced holes density. In either capillary or reservoir system, the ratio of reactivity to ionic diffusion determines the optimal condition for the reaction rate [12].

It is also revealed that large improvements in the resolution could be achieved if we could find an electrolyte in which the reaction velocity is an optimal. Since the resolution is not being limited by the intrinsic lateral diffusion of the holes between where they are generated and the surface, but rather by the diffusion that occurs in the region of high concentration that forms at the surface due to the low reaction velocity.

CHAPTER 7 FUTURE WORK

In the study of the photo-induced electrochemical etching or plating on the semiconductor surface, we have introduced the phenomena and relation of the photo-carrier and electrolyte concentration to the etching mechanisms, as well as, the external applied potential effect. It is easy to obtain the submicron feature resolution by varying the incident angle or optical source wavelength. Also, the fabrication steps have been greatly reduced.

We suggest that in the future works on the photo-induced electrochemical etching or plating on the semiconductor of

1. Research of various useful patterns to be imaged on the semiconductor surface.
2. Improvement of the modulation amplitude of the grating produced by looking for an optimal reaction velocity electrolyte composition, without losing the grating quality.

APPENDIX A

A-1 General Physical Constants.

Quantity	Symbol	Value
Elementary charge	q	1.602×10^{-19} [C]
Boltzmann Const.	k	8.620×10^{-5} [eV/K]
		1.3806×10^{-23} [J/K]
Avogadro number	NA	6.023×10^{23} [molec/Mol]
Electron volt	eV	1.60218×10^{-19} [J]
Thermal Voltage at 300 K	kT/q	.0259 [V]

A-2 Conversion Factors-units.

1 Å = 10^{-10} m = 10^{-4} μm

1 A = 1 C/s

1 eV = 1.60218×10^{-19} J

1 J = 1 N-m

1 W = 1 J/s

1 N = 1 kg-m/s^2

1 F = 1 C/V

A-3. InP Important physical properties/data.

1. Lattice constant : 5.869 Å

2. Bandgap E_g : 1.35 eV at 300°K (el)

   1.26 eV at 300°K (op).

3. Direct band

4. Mobility μ_n : 4600 [cm^2/ V sec.]

   μ_p : 150 [cm^2/ V sec.]

5. Dielectric const. 12.4

6. Absorption Coeff. α : 2.28 X 10^5 [cm^{-1}] at λ = 441.6 nm

   6.11 X 10^4 [cm^{-1}] at λ = 632.8 nm

7. Reflective index n : 3.833 at λ = 443 nm

   3.472 at λ = 563 nm

8. Crystal structure : Zincblende.

9. Diffusivity [cm^2/sec.] D_n : 119.14

   D_p : 3.88

10. Mass m_e : 0.077 m (el)

    m_e : 0.05 m (op)

    m_h : 0.64 m (el)

11. Carrier lifetime τ_p : 2.0 x 10^{-6} ~ 2.5 x 10^{-7}

    τ_n : 1.7 x 10^{-3} ~ 2.2 x 10^{-3}

A-4. Basic Dimension

Mass : [M]

Length : [L]

Time : [T]

Current : [A]

Temp. : [K]

A-5. Etching Dimension Consideration.

1. $$\frac{\partial}{\partial t} C = \frac{1}{q} \frac{\partial}{\partial y} J_c - \alpha_1\ p\ C$$

$$[L^{-3}\ T^{-1}] = [A^{-1}\ T^{-1}]\ [A\ L^{-2}]\ [L^{-1}] - [L^{2}\ T^{-1}]\ [L^{-2}]\ [L^{-3}]$$

$$= [L^{-3}\ T^{-1}] - [L^{-3}\ T^{-1}]$$

2. $$\frac{\alpha_2\ p\ C}{kT/q} \longrightarrow [\ \alpha_2\ ] = [M\ L^{2}\ A\ T^{-3}]\ [L^{2}]\ [L^{3}]$$

$$= [M\ A^{-1}\ T^{-3}\ L^{7}]$$

3. $$\beta = \frac{\alpha_2\ J_o\ \lambda}{kT} = \frac{[M\ A^{-1}\ T^{-3}\ L^{7}]\ [A\ L^{-2}]\ [L^{-1}]}{[M\ L^{2}\ T^{-2}\ ]}$$

$$= [L^{2}\ T^{-1}]$$

4. $$R = C1\ \alpha_1\ p\ C$$

$$= [L^{4}]\ [L^{2}\ T^{-1}]\ [L^{-2}]\ [L^{-3}]$$

$$= [L\ T^{-1}]$$

B. Ellipsometric measurement.

The oxide thin film on the specimen surface is a figure of merit in the etching business. So it is important to know the oxide layer film characteristic length in order to control the etching process. Since it is very thin layer (in the order of angstrom), the measurement is of critical and one of the convenient and accurate methods is the *ellipsometric*, in which the measurements are based on the changes of the optical polarization state as the light is reflected from the thin film surface.

The basic operation of the ellipsometer is shown as Fig. B-1. The parameters obtained from the ellipsometric measurement are based on the operation mode configuration, mostly are the real angle φ, Δ (most often), and δ (special case). Usually, the linearly polarized monochromatic light is incident at some definite angle onto the specimen, after reflected from the specimen the light turns out to be elliptically polarized. If the parameters characterizing the substrate ambient and light are known, then the optical characteristics of the film can be studied. The polarization state of the flux prior reflected from the specimen is determined by the polarizer, and the polarization state after reflection is measured by the analyzer. The resultant intensity is converted into electrical form by the photomultiplier detector. It is known from the snell's law that the cosine of the reflection angle is :

$$\cos \psi_2 = [1 - (\frac{n1}{n2} \sin \psi_1)^2]^{1/2}$$

The ratio of the normal and tangential total reflection coefficient is defined as ρ and given by :

$$\rho = \frac{Rp}{Rs} = \frac{(rp^{1,2} + rp^{2,3} e^{i2D})(1 + rs^{1,2} rs^{2,3} e^{i2D})}{(1 + rp^{1,2} rp^{2,3} e^{i2D})(rs^{1,2} + rs^{2,3} e^{i2D})}$$

$$= e^{i\Delta} \tan \varphi$$

where

$$D = \frac{2\pi d}{\lambda} (n_2^2 - n_1^2 \sin^2\psi_1)^{1/2}$$

with d is the film thickness, and the film reflection index can be calculated from :

$$n_3 = n_1 \tan \psi_1 [1 - \frac{4\rho \sin^2\psi1}{(1 + \rho)^2}]$$

The calculation is quite complicated and required several repetitions for accuracy. The computer numerically approaches is used to solve the above equation.

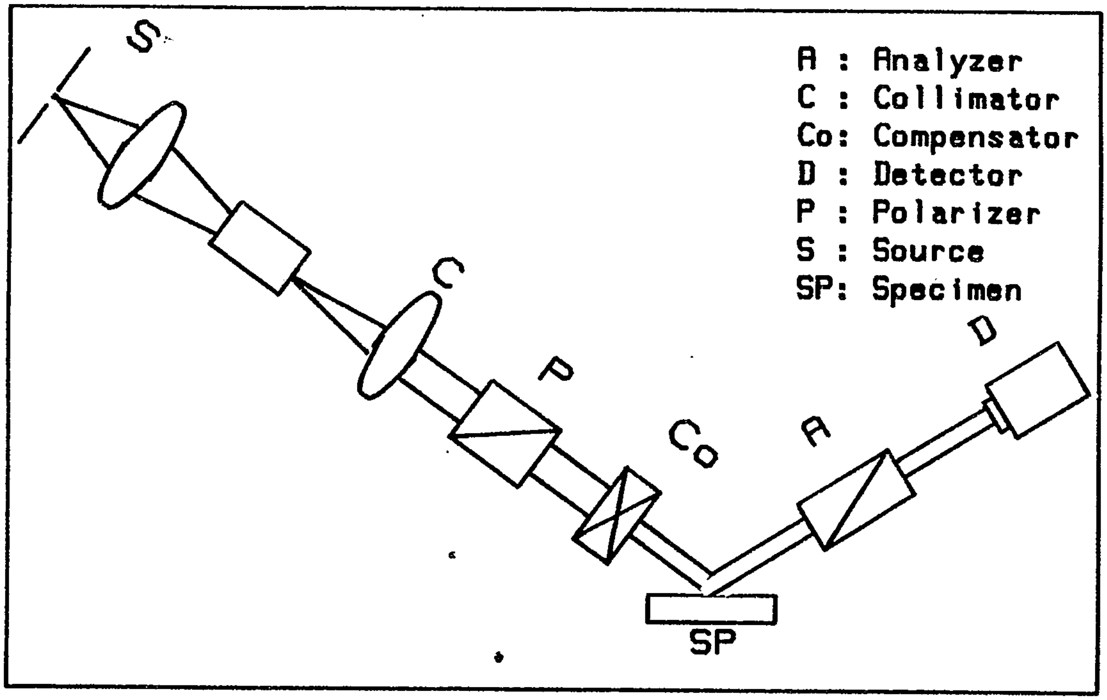

Fig. B-1 A Schematic Diagram of an Ellipsometric Measurement.

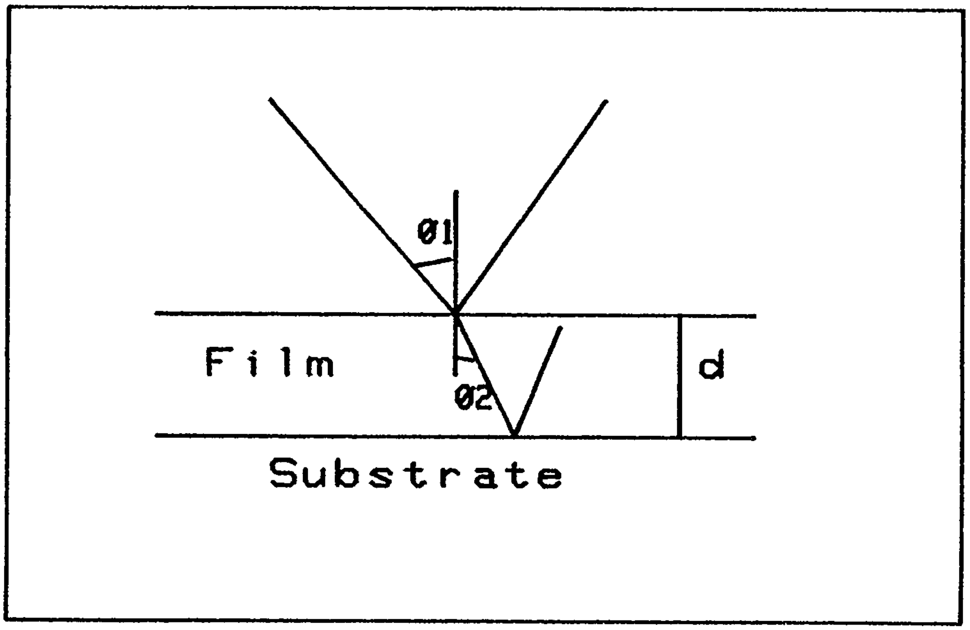

Fig. B-2 A Typical Reflection of an Ellipsometric Configuration

C. Computer Simulation Algorithms

```
**********************************************************
*    Program calculating surface effect                  *
*    external biasing field and electrolyte concentration *
**********************************************************
Variable $\phi_1$, $V_{ext}$, $C_o$, $\bar{C}_o$, $G_p$, $C_{ss}$, $I_i$, $\alpha_1$, d, layer.
Constant $\Delta\mu$, $\phi_o$, $\phi_q$, $\lambda$, $\alpha$, $\lambda_c$, $\tau_p$, $\nu$,
         q, h, c, $n_e$, KT, Alpha2
Begin;
     *****************************************************
     *  Generating alpha0, alpha1, beta, and ps parameters *
     *  and grating period for a certain incident angle $\theta_i$ *
     *****************************************************
     alpha0 = alpha2/$\phi_q$
     Alpha1 = depend on the electrolyte composition
     beta = (alpha2*$J_o$*$\lambda_c$)/($\phi_q$*q)
     d = $\lambda$/(2*$n_e$*sin$\theta_i$)
     $G_p$ = ($\alpha$*$I_i$)/($h\nu$)*exp(-$\alpha$*y)*(1+cos((2*$\pi$*x)/d)))
     ps = $G_p$*$\tau_p$
     readln ($C_o$)
     begin;
        readln ($V_{ext}$)
        $\phi_1$ = $\Delta\mu$*C-$V_{ext}$-$\phi_o$
        $\rho$ = [1+exp(-$\phi_1$/$\phi_q$)]
           if $V_{ext}$ < > 0
          ****************************************
          *  external biasing field effect       *
          ****************************************
          $C_{ss}$ = (beta/alpha1)*$\bar{C}_o$*exp(-alpha0*ps*$\bar{C}_o$)
          R = C1*alpha1*ps*$C_{ss}$*(1-$\rho$)
          R = R+.05
          T = 1/R
          writeln ($V_{ext}$,T)
          plot ($V_{exr}$,T)
          $C_o$ = $C_o$+0.0001
    end;
else;
begin;
readln (layer)
     if layer < 10 $\mu$m
     *********************************
     *   capillary system            *
     *********************************
     $C_{ss}$ = -[ln(alpha1/beta)/ps*alpha0)]
     R = C1*alpha1*ps*$C_{ss}$*(1-$\rho$)
     R = R+.05
     T = 1/R
     writeln ($C_o$,T)
```

```
          plot (Co,T)
          Co = Co+0.0001
     end;
     else;
          ************************************
          *   reservoir system               *
          ************************************
          Css = (beta/alpha1)*C̄o*exp(-alpha0*ps*C̄o)
          R = C1*alpha1*ps*Css*(1-ρ)
          R = R+.05
          T = 1/R
          writeln (Co,T)
          plot (Co,T)
          Co = Co+0.0001
     end;
end;
```

Bibliography.

[1]. S.M. Sze. "Semiconductor devices, physics and technologies".

[2]. Yu I. Ostrovsky, M.M. Butnsov, G.V. Ostrovskaya, "Interferometry by holography", Springer Ser. Opt. Sci., Vol.20 (Springer, Berlin, Heidelberg, New York 1980).

[3]. F.W. Ostermeyer,Jr., P.A. Kohl, and R.M. Sum, "Hole transport equation analysis of photoelectrochemical etching resolution". J.Appl.Phys. 58 (11), 4390, 1985.

[4]. L. Bäcklin, "Photoelectrochemical laser interference etching for fabrication of 235nm diffraction grating on InP". Elec.Lett, 23(12), 657, 1987.

[5]. A.E. Willner, D.V. Podlesnik, H.H Gilgen and R.M. Osgood, Jr., "Photobias effect in laser controlled etching of InP". Appl.Phys.Lett. 53(13), 1198, 1988.

[6]. S. Mottet and L. Henry. "Photochemical microetching of GaAs." Elec.Letts. 9(20), 919, 1983.

[7]. D.P. Kern, P.J. Coane, P.J. Houzego, and T.H. Chang. "Practical aspects of microfabrication in the 100nm region". Solid State Tech., 27(2), 127, 1984.

[8]. A. Guivarc'h, H. L'Haridon and G. Pelous. "Chemical cleaning of InP surfaces : Oxide composition and electrical properties". J.Appl.Phys. 55(4), 1139, 1984.

[9]. H.Kolgelnik, "Symposium on Modern Optics", edited by J.Fox. (Polytechnic, NY. 1967), p.605.

[10].P.A. Kohl, C. Wolowodiuk and F.W. Ostermeyer, Jr. "The

Photoelectrochemical Oxidation of (100), (111), and ($\overline{111}$) n-InP and n-GaAs. J.Electrochem.Soc. 130, 2288, 1983.

[11].J.E. Bjorkholm and L. Eichner. "Monitoring the growth of nonuniform gratings written holographically by gaussion laser beams". J.Appl.Phys 57, 2402, 1985.

[12].H. Grebel, B Iskandar and K.G. Sheppard. "The Effect of Non-Linear ion Transport on the rate of laser-induced electrochemical etching of semiconductor" to be published in J.Appl.Phys, 1989

[13].Yen, H.V., Nakamura, M., Garmire, E., Somekh, S., and Yariv, A., "Optically pumped GaAs waveguide lasers with a fundamental 0.11μm corrugation feedback". Opt.Commun., 9, 35-37, 1973.

[14].J.L. Vossen and W. Kern. "Thin film processes" Academic Press (1978) p.411.

[15].R.M. Lum, F.W. Ostermeyer, Jr., P.A. Koh;, A.M. Glass and A. Ballman. "Improvements in the modulation amplitude of submicron gratings produced in n-InP by direct photoelectrochemical etching". Appl.Phys.Lett. 47(3), 269,1985.

[16].W.Schockley and G.L. Pearson. "Modulation of conductance of thin film of semiconductor by surface charges". Phys.Rev. 74, 232,1948

[17].H. Grebel, B. Iskandar and K.G. Sheppard. "Photoelectrochemical etching of n-InP in a thin film cell". To be published in Appl.Phys.Lett. 1989.

[18].V. Svorcik, V. Rybika and V. Myslik. "Laser-stimulated etching of n-type semiconductor". Phys.Stat.Solid. (a) 106, K36, 1988.

[19].J.W. Goodman. "Introduction to fourier optics".